Bubble Nucleation to All Orders

Andreas Ekstedt*, a, b c

a: Department of Physics and Astronomy, Uppsala University, P.O. Box 256, SE-751 05 Uppsala, Sweden

b: II. Institute of Theoretical Physics, Universität Hamburg, D-22761, Hamburg, Germany

c: Deutsches Elektronen-Synchrotron DESY, Notkestr. 85, 22607 Hamburg, Germany

January 20, 2022

Abstract: This paper extends classical results by Langer and Kramers [1–3] and combines them with modern methods from high-temperature field theory [4–8]. Assuming Langevin dynamics, the end-product is an all-orders description of bubble-nucleation at high temperatures. Specifically, it's shown that equilibrium and non-equilibrium effects factorize to all orders—the nucleation rate splits into a statistical and dynamical prefactor. The derivation clarifies, and incorporates, higher-order corrections from zero-modes [9–11]. The rate is also shown to be real to all orders in perturbation theory. The methods are applied to several models. As such, Feynman rules are given; the relevant power-counting is introduced; RG invariance is shown; the connection with the effective action is discussed, and an explicit construction of propagators in an inhomogeneous background is given. The formalism applies to both phase and Sphaleron transitions. While mainly focused on field theory, the methods are applicable to finite-dimensional systems. Finally, as this paper assumes an effective Langevin description [4–7, 12–14], all results only hold within this framework.

1 Introduction

The observation of gravitational waves is a game-changer, granting us new eyes to gaze at the cosmos [15–18]. There is now a real chance of glimpsing phase transitions mere nanoseconds after the Big Bang. Depending of course on the phase transition in question. Contrary to continuous phase transitions, a first-order transition can leave tracks in the gravitational wave spectrum. Coupled with the possibility of Baryogenesis—thus potentially explaining the observed Baryon asymmetry [19–22]—these types of transitions beam with promise. So what differentiate these transitions from, say, second-order transitions? First-order transitions occur via nucleating bubbles [1, 3, 23–26]. The interior of these bubbles is permeated by a true vacuum; the outside stuck in a metastable state. And once

* andreas.ekstedt@desy.de

these bubbles expand they can generate gravitational waves via collisions and turbulence in the primordial plasma [27–31].

Yet it's unclear if such phase transitions actually occurred in our cosmological history, not to mention whether upcoming experiments can detect them [32–35].

Answering these questions requires inter-field expertise.

Indeed, from the theory side alone there's a need of both model building [36–45] and theoretical calculations [46–56]. Model building to identify attractive models; calculations to test their mettle. Therein lie the crux: Theoretical tools are, as yet, in their infancy. For there are ample uncertainties in describing the rate-of-production, and successive growth, of nucleating bubbles [17, 57–60]. Let alone determining if a first-order transition occurs at all [50, 52, 53]. Some of these problems are solved [17, 57, 61, 62], but a firm understanding of bubble-nucleation remains elusive.

And it's clear that tethering data to specific models requires precise calculations. Theoretical uncertainties for gravitational-wave production must be under control. And known. Leading-order results here give but an indication. Higher-order corrections provide much-needed cross-checks. This is especially relevant because higher-order corrections, for the rate, often dwarf naive expectations.

To that end, this paper vies to push bubble nucleation past leading order. To develop tools for calculating the rate in any model, and to improve gravitational-wave predictions.

The main result of this paper for the nucleation rate is

$$\Gamma = A_{\text{dyn}} \times A_{\text{stat}} \tag{1.1}$$

Here A_{dyn} accounts for non-equilibrium effects and A_{stat} for equilibrium ones. These factors are known as the dynamical and statistical prefactor respectively, and they can be calculated order-by-order in perturbation theory. Equation 1.1 is derived in Section 3, and applied to a real-scalar model in Section 5. Crucially all derivations assume a classical Hamiltonian system. And all higher-order corrections are only treated within this system. See [4–7, 12–14] for the details and applicability of this effective description.

I also want to stress that formulas akin to Equation 1.1 have been suggested before [1, 23, 61, 63, 64]. These have however only been proved to leading order. And it's unclear from past literature how higher-order corrections should, even in principle, be included.

This paper fills these gaps. In particular, the nucleation rate is derived from first principles, and the factorization in Equation 1.1 is proved to all orders. Furthermore, it is shown step-by-step how to include perturbative corrections at higher orders. This includes deriving Feynman rules for calculating the statistical and dynamical prefactors, and consistently treating zero-modes.

The derivation is alloyed by explicit calculations showing that the rate is renormalization-scale invariant to two-loops; that the rate is real to all orders; and the connection with the effective action.

Finally, Section 6 delineates subtle issues that arise in perturbation theory. These includes calculating propagators numerically, treating zero-modes at higher orders, and using a consistent power-counting.

2 Uncertainties for Thermal Escape

Before doing any explicit calculations, it is fitting to review existing methods and see their virtues and vices.

When studying thermal escape in field theory, one looks for solutions to the classical equations of motion. Not any solution, rather, these *bounce* solutions obey particular boundary conditions and are the field-theory equivalent to saddle points [24–26]. The energy of this saddle point—in three dimensions denoted S_3—determines the probability to jump from a metastable state to a lower-energy state. These jumps result in nucleating bubbles.

An approximation for the nucleation rate at high temperatures is [23, 63, 64]

$$\Gamma \approx AT^4 e^{-S_3/T} \tag{2.1}$$

Naively one expects the exponent to dominate. So when the transition happens, around $S_3 \approx 140T$ [17, 18], the exponential prefactor should be sub-leading.

Equation 2.1 does however have its share of flaws. The most glaring is that S_3 depends on the renormalization-scale, which introduces significant uncertainties [58]. Second, and more sinister, the prefactor can dominate the exponent [46, 47, 61]. Third, the form of Equation 2.1 ignores non-equilibrium physics [1, 3].

2.1 Renormalization-Scale Dependence

Scale dependence is a solved problem. Yet if one is not careful, there can be large logarithms at high temperatures. Indeed, even equilibrium calculations involving the effective potential are tricky. In particular, at one-loop and beyond there are logarithms of the form $\log \frac{\mu^2}{T^2}$ and $\log \frac{\mu^2}{m^2}$. Here m^2 is an arbitrary mass and is expected to be of order $m^2 \sim g^2 T^2$ at the transition. So whatever choice of μ, one logarithm is large. The solution is to integrate out modes with momenta $k \sim T$ [46, 48, 49]. The resulting effective theory lives in three spatial dimensions, and matching this dimensionally reduced theory to the original 4-D theory resums $\log \frac{\mu^2}{T^2}$ terms. Applying these considerations to the rate removes some scale-dependence, leaving only dependence on the 3-D scale μ_3. The dependence on μ_3, while large, is much milder than in the original 4-D theory.

In short, for robust results one should use a dimensionally reduced theory when calculating the rate [46, 47, 61, 65].

2.2 Size of the Exponential Prefactor

Another problem is that the assumed sub-leading exponential prefactor A is not sub-leading nor really a prefactor.

There are several contributing factors. For clarity, write the rate as

$$-\log \Gamma \sim S_3/T - \log A. \tag{2.2}$$

For thin-walled bubbles—meaning a small energy-difference between the vacua—the first term scales as $S_3 \sim \epsilon R^3$ [3, 24, 26, 63, 66]; ϵ is here the energy-difference between the metastable and true vacuum, and R is the bubble-radius scaling as $R \sim \epsilon^{-1}$: $S_3 \sim R^2$. Now, $\log A$ can be estimated as the one-loop difference in energy (the effective potential) between the true and metastable state.[1] In the thin-wall limit this amounts to

$$\log A \sim R^3 \left[V_{\text{eff}}(\phi_{\text{true}}) - V_{\text{eff}}(\phi_{\text{false}})\right] \sim R^3 g^a, \tag{2.3}$$

for some a. A vector-boson, for example, contributes $\log A \sim -R^3 \frac{\phi_{\text{TV}}^3 g^3}{12\pi}$ where ϕ_{TV} denotes the true vacuum.

The above discussion shows that the calculation breaks down for $R \sim g^{-a}$. Thus perturbative calculations can't be trusted in the thin-wall limit.[2]

It is also possible for A to be of the same order, or larger, than the exponent if there are heavy particles in the theory. For example, if a particle with mass M talks with the Higgs the prefactor scales as $\log A \sim M^{3/2}$. The solution is to integrate out these heavy particles before calculating the rate [47, 57, 61, 65]. Though, one should still be careful unless these particles are parametrically heavy.

All in all, higher-order corrections can be, and generally are, larger than naively expected. This is true even away from the strict thin-wall limit. Although this is hidden in Equation 2.1, explicit calculations have confirmed this behaviour [46, 47, 57, 65].

In general one should be wary of relying on perturbative estimates, or the thin-wall limit, when studying thermal escape and tunneling.

2.3 Non-Equilibrium Dynamics

Thermal escape is a non-equilibrium process. As such, damping and related effects are important [1, 23, 63]. These details are ignored if Equation 2.1 is used without calculating the prefactor. What's worse, classical calculations of thermal escape indicate that the saddle-point approximation breaks down for small damping [68]. This makes using existing formulas [23, 64] precarious at best.

These three problems—not to mention gauge dependence [57, 60, 65]—result in order-of-magnitude uncertainties for the rate. And these uncertainties propagate to gravitational-wave predictions [17, 58].

To see how and where Equation 2.1 fails, and how to alleviate the problems, I next discuss the physics behind thermal escape. This discussion is schematic and omits technical details, which are left for Sections 3, 4, and 5.

1 Explicit calculations confirm this [47, 67].

2 There are a few models that do work in the thin-wall limit. For example a real-scalar field with a $V(\phi) = m^2\phi^2 - g\phi^3 + \lambda\phi^4$ potential. Yet the moment vector fields, or Goldstone bosons, are present, the thin-wall limit breaks down.

2.4 Thermal Escape and Tunneling

While there are many similarities between tunneling and thermal escape, there are critical differences. At first glance the formulas look rather similar

$$\Gamma_{T=0} = \left(\frac{S_B}{2\pi}\right)^2 \left|\frac{\det([-\partial^2 + V''(0)])}{\det'[-\partial^2 + V''(\phi_b)]}\right|^{1/2} e^{-S_B} \tag{2.4}$$

$$\Gamma_{T\neq 0} = \frac{\lambda}{2\pi}\left(\frac{S_3}{2\pi T}\right)^{3/2} \left|\frac{\det([-\partial^2 + V''(0)])}{\det'[-\partial^2 + V''(\phi_b)]}\right|^{1/2} e^{-S_3/T} \tag{2.5}$$

where λ is the growth-rate of the bubble [1].

For tunneling, the rate is[3]

$$\Gamma_{T=0} = 2\mathrm{Im} e^{-S_{\text{eff}}}. \tag{2.6}$$

The effective action is here evaluated on a solution $\delta S_{\text{eff}}[\phi_b] = 0$. Essentially the tunneling rate comes from a saddle-point approximation. The functional determinant (one-loop contribution to S_{eff}) arises from fluctuations around the bounce, and higher-order terms in S_{eff} consist of vacuum diagrams in the bounce background [9,10]. Crucially the effective action is imaginary due to a negative eigenvalue.

The high-temperature formula looks alluringly similar to the tunneling one. Ignoring the prefactor, the determinant and exponent looks like the first terms of $e^{-S_{\text{eff}}/T}$, where S_{eff} is the effective action in three dimensions. A natural conjecture is [69,70]

$$\Gamma_{T\neq 0} = A_{\text{dyn}} \times 2\mathrm{Im} e^{-S_{\text{eff}}/T}, \tag{2.7}$$

The leading-order dynamical prefactor is $A_{\text{dyn}} = \frac{\lambda}{2\pi}$, and λ is normally taken as $\sqrt{|\kappa|}$, with κ being the only negative eigenvalue of $\delta^2 S_3[\phi_b]$.

Yet this is not quite right. For one there are no imaginary contributions at any stage in the calculation. For another, it's not the effective action that appears in the exponent. What's more, this formula does not include higher-order corrections to the dynamical prefactor.

Let's for the moment leave field theory behind, and look at a classical particle moving in three dimensions. Much of this discussion carries over to field theory.

Picture a metastable minimum at $\vec{x} = \vec{x}_S$, and another, lower-energy one, at $\vec{x} = \vec{x}_{\text{TV}}$. Furthermore, let's assume that these two minima are separated by a barrier. Lowest at say $\vec{x} = \vec{x}_B$. Without loss of generality I take $\vec{x}_B$ to lie in the x_1 direction.

Now, if this was a tunneling process, the particle would start at the metastable minimum and go through the barrier with some probability. The position of the barrier is here secondary as the particle also pays with kinetic energy whichever path it chooses. The most likely path of escape, the bounce, has a negative eigenvalue, which gives an imaginary energy. The rate is identified with $\Gamma = -2\mathrm{Im}\mathcal{E}$.

But the picture is different for thermal escape. Here the particle does not travel through the barrier—it jumps over it. That is, the probability for the particle to have an energy

3 I here neglect subtleties related to zero modes [9,10]. These are discussed in Section 5.2.

E is proportional to $e^{-E/T}$. So the likeliest direction of escape is along $\vec{x}_B$, with naive probability $\Gamma \sim e^{-V_B/T}$, where $V_B = V(x)|_{x=\vec{x}_B}$. This is almost right. The particle can also escape close-by $\vec{x}_B$ by moving slightly in the x_2 or x_3 directions, paying in probability as it does so.[4]

A better approximation is $\Gamma \sim \int_{x=x_1} dx_2 dx_3 e^{-V(x)/T}$. Crucially only variations in orthogonal directions to $\vec{x}_B$ are included this integral. The rate is real as there's no integration in the concave x_1 direction. This contribution from the Boltzmann factor is the statistical prefactor.

What about non-equilibrium physics? When the particle jumps over the barrier, it first needs to get sufficient energy to escape, and then move to the other side. If the *negative* curvature (κ) in the concave direction is large, the probability to get moving over the edge is naturally big. Likewise, for large damping (η) the particle has a harder time to get going. This is the physical reason for the leading-order dynamical prefactor: $A_{\text{dyn}} = \frac{|\kappa|}{2\pi\eta}$.

Note that the flow across the barrier is only sensitive to deviations from thermal equilibrium. Indeed, in thermal equilibrium the system is static.

Intuitively the Boltzmann factor describes the probability to jump up to, and the dynamical factor describes the flow from, the barrier. To leading order this flow is just in the concave direction, while higher-order corrections make the flow veer down the barrier from orthogonal directions.

Although schematic, this discussion illustrates where tunneling and thermal escape fundamentally differ: Tunneling involves the particle going through the barrier via some path, thermal escape involves the particle escaping where the barrier is lowest.

In essence, it doesn't matter that V is concave in the x_1 direction because we should only integrate in orthogonal directions to x_1 when calculating the rate. And no imaginary terms can appear in the saddle-point approximation.[5]

These considerations motivate the main result of this paper

$$\Gamma_{T\neq 0} = A_{\text{dyn}} e^{-\overline{S}_{\text{eff}}}, \tag{2.8}$$

where the effective action omits any corrections from the negative-eigenvector direction. This means that there are no negative eigenvalues in the Gaussian integral, and that this effective action is real to all orders.

Strictly speaking this holds only for large damping. And an equivalent formula for generic damping is given in Section 4. In addition, the effective action in Equation 2.8 contains non-trivial corrections from zero modes as discussed in Section 5.2.

In the next section I derive Equation 2.8 for an overdamped system; an equivalent derivation for general damping is given in Section 4. The complete nucleation rate is given in Section 5.6.

4 This discussion assumes an overdamped system, and ignore kinetic contributions to the energy. See Section 4 for a discussion of the general case.

5 This has been previously observed in [61, 68, 71]. However, care must be taken for generic damping. And away from the strict overdamping limit the integral should not be done at the saddle point. Yet the decay rate is still real for general damping coefficients, but the reason is more subtle. See Section 4.

3 The Nucleation Rate

In this section I show how to calculate the nucleation-rate to arbitrary order in perturbation theory. To make the derivation cleaner, I first consider a system with n degrees of freedom, indexed by i. Translating everything to field theory is straightforward (see [71]), but all results are applicable to finite-dimensional systems. Section 5 gives a dictionary for converting all formulas to field theory.

To save ink an overdamped system is used. In essence a large damping suppresses momentum fluctuations, which in practice means that the Boltzmann factor does not contain kinetic terms.

While not generic, an overdamped system makes the physics transparent. This coupled with that the overdamped case is appropriate when describing phase transitions in the Standard Model and beyond [4, 7, 8], makes this limit appropriate. The steps are similar for the general case. Differing only by longer intermediate formulas, which are given in Section 4.

To start off, note that the calculation of the nucleation rate is classical. This follows because field theory is, to first approximation, classical at high temperatures [4–8]. This is indicated by the Boltzmann factor

$$n(\omega) = \frac{1}{e^{\omega/T} - 1}. \tag{3.1}$$

At high temperatures $T \gg \omega$, the occupation number is large: $n(\omega) \approx T/\omega \gg 1$. Equivalently, the system is classical if the thermal-wavelength is small: $\lambda_T^{-1}\lambda_{\text{dB}} \sim \frac{T}{\omega} \gg \hbar$.

However, although nucleation occurs at low energies, large energy modes with $\omega \sim T$ still contribute. Through loops if nothing else. Luckily these high-energy modes are fast and average out to give an effective damping and thermal noise [4].

In this Section I don't derive the damping, rather, the damping is taken as a free parameter. See [4–8] for explicit calculations of the damping.

3.1 Classical Nucleation Theory

This Section reviews classical Nucleation theory. I want to stress that the results in this first subsection are long known [1, 2, 68, 71, 72], and I only include the details needed to go to higher orders.

The Einstein summation convention is used for indices i, j, k, l. The vertical position of these indices is unimportant.

Consider the Fokker-Planck equation for a system with large damping (also known as the Smoluchowski equation) [73, 74]

$$\partial_t P = -\partial_i J^i, \quad J^i = -\left[\frac{1}{\eta} P \partial_i V + \frac{T}{\eta}\partial_i P\right]. \tag{3.2}$$

Here $V(x)$ is a generic potential and η represents the damping.[6]

6 It is assumed that all components $[x^i]$ have the same damping η; one could imagine cases aplenty with different damping for different components. As for example happens for the weak gauge fields and the Higgs. This

The function $P(x,t;x_0,t_0)$ is the probability to find the particle at a position x, given that it was at x_0 at time t_0. Then, if P is initially localized to a metastable configuration—defined by the potential V—we can ask what's the probability to find the particle at a lower-energy state.

Determining P as a function of t is an Herculean task, yet it's enough to know P where the particle is likely to escape—at the barrier. The rate can be approximated by the probability flow, defined by J^i, across this barrier [1, 2, 68]:

$$\Gamma = \frac{\int_{\text{barrier}} d\vec{S}\cdot\vec{J}}{\int_{\text{metastable}} d^n x P}. \tag{3.3}$$

The rate can then be calculated analytically be using a trick due to Kramers. The idea is to introduce artificial sources and sinks guaranteeing a static P [1, 2, 68, 71]. So the problem is reduced to solving the static Fokker-Planck equation. After the equation is solved, and we have our current, the sinks and sources can be removed. This is known as the flux-over-population method. It should be mentioned that this method fails for underdamped systems [68].

Therefore consider a time-independent solution around the metastable state, say at $\vec{x}=\vec{x}_S$. The (static) equilibrium solution is $P_0 = e^{-V(x)/T}$, which is the normal Boltzmann distribution and follows from Equation 3.2. Further, if close to the metastable point the potential is $V(x+x_S) = V_S + \frac{1}{2}x^i\omega_S^{ij}x^j + \ldots$, the normalization factor $\int_{\text{metastable}} d^n x P$ is given by the usual saddle-point formula.[7] Note that the probability current, and hence the rate, vanish identically if $P = e^{-V(x)/T}$. This is because the system would be at thermal equilibrium.

Next, the idea is to determine P close to the barrier separating the two phases. That is, we want to find P close to a saddle point.

Before moving on, let's note two approximations that will be used. First, we assume that the surface integral in Equation 3.3 is dominated by the saddle point. Second, we assume that the surface can be approximated as a surface normal to the saddle point.

That said, close to the saddle point we again want to solve the static system. However, the solution can not simply be an equilibrium distribution. Reason being that, by assumption, the distribution is localized to the metastable state; the probability to find the particle at the true minima should be tiny.

Thus following Langer one makes the ansatz $P = \zeta(\vec{x})e^{-V(x)/T}$. The function $\zeta(\vec{x})$ describes deviations from thermal equilibrium and behaves as

$$\lim_{\vec{x}\to\vec{x}_S} \zeta(\vec{x}) = 1, \tag{3.4}$$

$$\lim_{\vec{x}\to\vec{x}_{\text{TV}}} \zeta(\vec{x}) = 0. \tag{3.5}$$

complication does not alter the final result. See Appendix A.

7 Higher-order corrections in V can be included as perturbations, for example by using Feynman rules in a homogenous background [62, 75].

Plugging this ansatz into Equation 3.2 one finds

$$T\partial_i\partial^i\zeta - \partial^i V\partial^i\zeta = 0. \tag{3.6}$$

Next, to solve the equations, assume that the saddle point is at x_B^i. At this point the potential is $V(x_B + x) = V_B + \frac{1}{2}x^i\omega^{ij}x^j$. Hence

$$T\partial_i\partial^i\zeta - x^i\omega^{ij}\partial^j\zeta = 0. \tag{3.7}$$

This equation can be solved with the ansatz $\zeta(\vec{x}) = \zeta(u)$, where u is a linear combination of $\vec{x}$. Namely, $u = \overline{U}^i x_i$. Then

$$T\overline{U}^2\zeta''(u) - x_i\omega^{ij}\overline{U}^j\zeta'(u) = 0, \tag{3.8}$$

where $\overline{U}^i$ must be an eigenvector of ω^{ij} for consistency. That is

$$\omega^{ij}\overline{U}^j = \kappa\overline{U}^i. \tag{3.9}$$

We are free to normalize $\overline{U}^i$ as we see fit, and we might as well choose $\overline{U}^2 = 1$. The solution to Equation 3.9 is [1, 68]

$$\begin{aligned}\zeta(u) &= \frac{1}{\sqrt{2\pi|\alpha|}}\int_u^\infty du' e^{-u'^2/(2|\alpha|)}, \\ \alpha &= \frac{T}{\kappa}.\end{aligned} \tag{3.10}$$

The boundary conditions for $\zeta(u)$ force $\kappa < 0$, and so $\overline{U}^i$ is the eigenvector corresponding to a negative eigenvalue. And κ is the curvature in the concave direction. So the deviation from equilibrium only depends on how far we move in the negative-eigenvalue direction.

Given $\zeta(u)$, the current is

$$J^i = -\left[\frac{1}{\eta}P\partial_i V + \frac{T}{\eta}\partial_i\right]P = -\overline{U}^i\frac{T}{\eta}\zeta'(u)P_0, \tag{3.11}$$

where $P_0 = e^{-V(x)/T}$.

To find the rate we integrate the current on a surface normal to $u = 0$. This gives the rate[8]

$$\Gamma = \int_{u=0} d^n x\overline{U}^i J^i = \frac{1}{\eta}\int d^n x\int_{-\infty}^{\infty}\frac{dk}{2\pi}\frac{1}{\sqrt{2\pi|\alpha|}}e^{iku - V(x)/T}, \tag{3.12}$$

where to leading order $V(x + x_B) \approx V_B + \frac{1}{2}x_i\omega^{ij}x_j$.

There are a number of sanity checks to this formula. First, the rate does not depend on the orientation of the surface as long as it contains $\vec{x}_B$. Further, the rate is manifestly

8 Here, following [68], the delta function has been rewritten as $\delta(u) = \frac{1}{2\pi}\int_\infty^\infty dk e^{iku}$. This makes no difference at this stage, since one could just set $u = 0$ by hand. Yet later calculations are greatly simplified by this trick.

real because $u = 0$ projects out the negative eigenvalue.

Doing the integrations, and being cavalier about factors of 2π, one finds [1, 68]

$$\Gamma = \frac{|\sqrt{\kappa}|}{2\pi\eta}\left[\bar{\det}'\omega\right]^{-1/2} e^{-\frac{V_B}{T}}, \tag{3.13}$$

where $\bar{\det}'$ means that all negative and zero eigenvalues are excluded.[9]

Crucially $u = 0$ excludes the negative-eigenvalue direction, and so the determinant is manifestly real. This is contrary to the tunnelling case where the negative eigenvalue gives the determinant a complex phase.

Normalizing with the metastable state gives the known result [1, 68, 71]

$$\Gamma = \frac{|\sqrt{\kappa}|}{2\pi\eta}\left[\frac{\bar{\det}'\omega}{\det\omega_S}\right]^{-1/2} e^{-\frac{(V_B - V_S)}{T}}. \tag{3.14}$$

I will throughout this paper refer to this as the leading-order rate.

Let's now dash ahead to higher-order corrections. There are two kinds. First, corrections to the dynamical prefactor come from including more terms for V in Equation 3.6. Second, the statistical prefactor receives corrections from additional terms in V via equation 3.12. To leading order

$$\Gamma = A_{\text{dyn}} \times A_{\text{stat}}, \tag{3.15}$$

$$A_{\text{dyn}} = \frac{|\sqrt{\kappa}|}{2\pi\eta} \quad \& \quad A_{\text{stat}} = \left[\bar{\det}'\omega\right]^{-1/2} e^{-\frac{V_B}{T}}. \tag{3.16}$$

Intuitively A_{dyn} incorporates deviations from thermal equilibrium, and A_{stat} corresponds to Boltzmann suppression.

As the next two sections show, the statistical prefactor consists of normal (exponentiated) vacuum diagrams; the dynamical prefactor, in field language, consists of operator insertions.

For brevity I leave the metastable normalization implicit. This normalization factor is straightforward to calculate via the effective potential [62, 75].

3.2 Corrections to The Statistical Prefactor

Consider the statistical prefactor. As mentioned, the negative eigenvalue does not cause any issues because everything is calculated at $u = 0$. Yet it's auspicious to not enforce this by hand. For one, all the calculations are easier to generalize to field theory. For another, it's easier to check explicit RG-invariance (see section 5.4).

To start off, consider the Boltzmann-like integral in Equation 3.12

$$Z[\overline{U}] = \int d^n x e^{iku - 1/T\frac{1}{2}\left(x_i \omega^{ij} x_j\right)}. \tag{3.17}$$

Integrating over k enforces $u = 0$, and I leave this integration for last.

9 I purposely ignore zero eigenvalues. These are discussed in Section 5.2.

Barring some subtleties with the negative eigenvalue, the integrals give

$$Z[\overline{U}] = \left[\det{}' \omega/(2\pi)\right]^{-1/2} e^{-\frac{1}{2}k^2 T \overline{U}^i \omega_{ij}^{-1} \overline{U}^j}. \tag{3.18}$$

There remains the snag that $\overline{U}^i \omega_{ij}^{-1} \overline{U}^j < 0$, so the integral over k formally diverges. Worse still, $\left[\det{}' \omega/(2\pi)\right]^{1/2}$ is imaginary because the negative eigenvalue is included. These problems are of course not really there since the negative eigenvalue is left-out by definition.

Being a bit more careful one can let $k \to -ik$ and do a Wick-rotation. This gives

$$Z[\overline{U}] = \left[|\det{}' \omega/(2\pi)|\right]^{-1/2} e^{\frac{1}{2}k^2 T \overline{U}^i \omega_{ij}^{-1} \overline{U}^j}. \tag{3.19}$$

We identify $Z[\overline{U}]$ as a generating function. And correlators can be calculated via

$$< x^i x^j > \equiv \int_{-\infty}^{\infty} dk \int d^n x x^i x^j e^{iku - 1/T\left(x_i \omega^{ij} x_j\right)} \equiv \int_{-\infty}^{\infty} dk (k)^{-2} \frac{\partial^2}{\partial \overline{U}^i \partial \overline{U}^j} Z. \tag{3.20}$$

So $Z[\overline{U}]$ is a generating function with a non-vanishing current.[10] In terms of Feynman diagrams this means that on top of usual diagrams, there are now diagrams with external-current insertions.

To see everything in action, consider the potential

$$V(x + x_B) = V_B + \frac{1}{2} x^i \omega^{ij} x^j + \frac{1}{4!} \lambda_4^{ijkl} x^i x^j x^k x^l. \tag{3.21}$$

The Feynman rules are

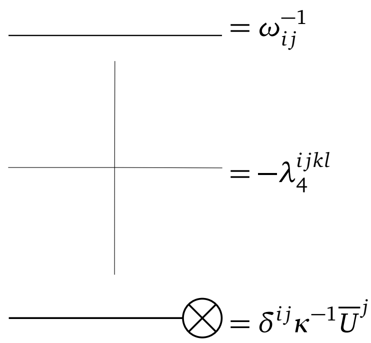

In addition, if there are $2n$ external-current insertions, the diagram picks up a factor $(-1)^n \kappa^n (2n-1)!!$. This last rule comes from integrating over k. Also, diagrams with an odd-number of current insertions vanish since $\int_{-\infty}^{\infty} dk k^{2n+1} e^{-k^2 A} = 0$.

At NLO the diagrams are[11]

10 If one is uncomfortable with treating $\overline{U}$ as general even though it's fixed as the negative eigenvector, it's possible to use $e^{iku} \to \int \frac{d^n \tilde{U}}{(2\pi)^n} \delta^{(n)}(\tilde{U} - \overline{U}) e^{ik\tilde{u}}$. All the steps are identical.

11 All of these diagrams must be of two-loop size since the last two diagrams have to remove the negative eigenvalue from the first. See Section 6.1 for the details.

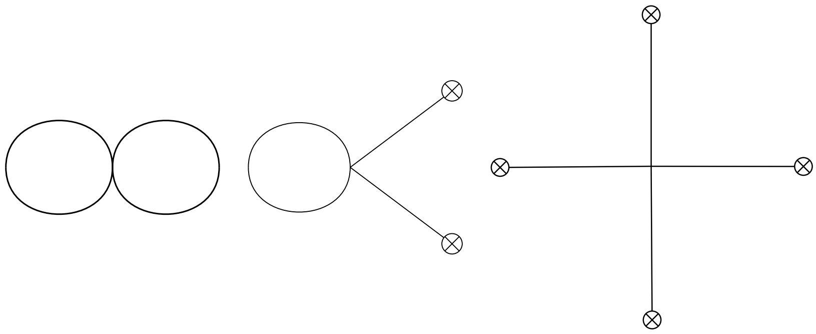

Using the Feynman rules above, the first diagram gives $-\frac{1}{8}\omega^{-1}_{ij}\omega^{-1}_{kl}\lambda_4^{ijkl}$; the second $\frac{1}{4}\kappa^{-1}\omega^{-1}_{ij}\overline{U}^k\overline{U}^l\lambda_4^{ijkl}$; and the third $-\frac{3}{4!}\kappa^{-2}\overline{U}^i\overline{U}^j\overline{U}^k\overline{U}^l\lambda_4^{ijkl}$.

The propagator can be written

$$\omega^{-1}_{ij} = \sum_a \frac{\overline{V}^i_a\overline{V}^j_a}{\lambda_a}, \tag{3.22}$$

where $\overline{V}^i_a$ are eigenvectors of ω^{ij} with eigenvalue λ_a. After using this form for ω^{-1}_{ij}, the last two diagrams just amounts to removing κ from the first. That is, the negative eigenvalue in an L-loop diagram, is removed by slicing L-loop diagrams open.

The above procedure carries over to field theory with ω^{-1}_{ij} replaced by a propagator. See Section 5.

All in all, the statistical prefactor is

$$A_{\text{stat}} = e^{-\bar{S}_{\text{eff}}}, \tag{3.23}$$

where $\bar{S}_{\text{eff}}$ denotes all vacuum diagrams omitting zero and negative eigenmodes.

I want to stress that this statistical prefactor is only correct in the overdamping limit. See Section 4 for the general case.

3.3 Corrections to The Dynamical Prefactor

With the statistical prefactor settled, let's turn to the dynamical one. Here I limit myself to the potential[12]

$$V(x+x_B) = V_B + \frac{1}{2}x_i\omega^{ij}x_j + \frac{1}{3!}\lambda_3^{ijk}x_ix_jx_k + \frac{1}{4!}\lambda_4^{ijkl}x_ix_jx_kx_l. \tag{3.24}$$

Including higher-order terms in V does two things. First, the Boltzmann factor $\sim \int_{u=0} d^nxe^{-V(x)/T}$ changes. This is encoded by the statistical prefactor. Second, the rate of flow across the saddle-point will change. This flow is controlled by deviations from thermal equilibrium, which is encoded in the dynamical prefactor.

12 The result for a potential of degree 6 is given in Appendix C.

That said, let's turn to the dynamical prefactor. Because Equation 3.6 describes the deviation from equilibrium, we need to find ζ to higher orders. Explicitly, we need to solve $T\partial_i^2\zeta - \partial_i V \partial^i \zeta = 0$ with the inclusion of λ_3 and λ_4 terms. The leading-order solution, denoted henceforth as ζ_0, is given in Equation 3.10.

While ζ_0 only depends on $u = \overline{U}^i x^i$, higher-order corrections depend on generic x^i. Yet the boundary conditions force $\zeta(\vec{x})$ to vanish as $u \to \infty$. We might as well enforce this directly with the ansatz

$$\zeta = \zeta_0(u) + \zeta_0'(u)\zeta_1(x) + \dots \tag{3.25}$$

The first term takes care of the boundary conditions, and all sub-leading terms vanish as $u \to \pm\infty$. It is assumed that $\zeta_1 = \mathcal{O}\left(\lambda_3, \lambda_4\right)$.

The equation for ζ_1 can be found by plugging 3.25 into Equation 3.6:

$$T\partial_i^2\zeta_1 + \partial_i\zeta_1\left[2\kappa u\overline{U}^i - \omega^{ij}x_j\right] + \kappa\zeta_1 = \left\langle \overline{U}x^2\right\rangle + \left\langle \overline{U}x^3\right\rangle. \tag{3.26}$$

To save ink I use the short-hand $\left\langle x^3\right\rangle \equiv \frac{1}{2!}\lambda_3^{ijk}x_i x_j x_k$ and $\left\langle x^4\right\rangle \equiv \frac{1}{3!}\lambda_4^{ijkl}x_i x_j x_k x_l$.

All homogenous solutions grow exponentially with u, or lead to inconsistencies, and so don't satisfy the boundary conditions ($\lim_{u\to\pm\infty}\zeta_0'(u)\zeta_1(\vec{x}) = 0$). This leaves only the particular solution.

Now, if we make a polynomial ansatz [in x^i], neither of the terms on the left-hand side of Equation 3.26 increase the polynomial's degree. Whence the ansatz go through the equations.

Next, to solve the equation it's apt to work in the eigenbasis of ω : $\omega^{ij}\overline{V}_a^j = \lambda_a \overline{V}_a^i$. That is, expand $x^i = u\overline{U}^i + \sum_a v_a \overline{V}_a^i$ where $v_a = \overline{V}_a^i x^i$. This basis is useful because $\overline{V}_a^i$ is orthogonal to $\overline{U}^i$ coupled with that $\omega^{ij}x_j$ reduces to a sum of eigenvalues. So the idea is to make a polynomial ansatz in u and v_a. Here, and after, I let a denote all eigenvalues barring the negative one. So λ_a does not include κ.

To get a feel for the solution, consider the 2-D case $(x^i) = (x^1, x^2)$ and ignore the $\left\langle x^4\right\rangle$ term for the moment. That is, take the potential

$$V(x + x_B) = V_B + \frac{1}{2}x_i\omega^{ij}x_j + \frac{1}{3!}\lambda_3^{ijk}x_i x_j x_k. \tag{3.27}$$

There are two eigenvectors: $\omega^{ij}\overline{U}^j = \kappa\overline{U}^i$ and $\omega^{ij}\overline{V}^j = \lambda_v\overline{V}^i$. These eigenvectors define $u \equiv \overline{U}^i x^i$ and $v = \overline{V}^i x^i$.

Expanding x^i in u and v gives

$$\left\langle \overline{U}x^2\right\rangle = u^2\left\langle \overline{U}^3\right\rangle + 2uv\left\langle \overline{U}^2\overline{V}\right\rangle + v^2\left\langle \overline{U}\overline{V}^2\right\rangle. \tag{3.28}$$

Since $\left\langle \overline{U}x^2\right\rangle$ is a degree 2 polynomial, the relevant ansatz is

$$\zeta_1 = A + B_1 u + B_2 v + C_1 u^2 + C_2 v^2 + C_3 uv.$$

Plugging this ansatz into Equation 3.26 and collecting terms one finds

$$\begin{aligned} &B_1 = B_2 = 0, && A = -2T(C_1 + C_2)/\kappa, \\ &C_1 = (3\kappa)^{-1}\left\langle \overline{U}^3 \right\rangle, && C_2 = (\kappa - 2\lambda_v)^{-1}\left\langle \overline{U}\overline{V}^2 \right\rangle, \\ &C_3 = 2\,(2\kappa - \lambda_v)^{-1}\left\langle \overline{U}^2\overline{V} \right\rangle. \end{aligned} \tag{3.29}$$

Note that most of the terms in ζ_1 are irrelevant. Reason being that the rate is given by $\int_{u=0} d^n x \overline{U}^i J^i \sim \int \overline{U}^i \partial_i \zeta_1|_{u=0}$. For the above example only the $C_3 uv$ term contributes since if the derivative (∂^i) hits anything else, that term is proportional to u or $\overline{U}^i\overline{V}^i$. Both which vanish. This holds in general: We only have to care about terms containing *one* factor of u.

With our artillery at the ready, consider the n-dimensional case. Including the quartic term in Equation 3.26, the ansatz is a polynomial of degree 3:

$$\zeta_1 = A + B_1 u + \sum_a B_a v_a + \ldots + u \sum C_a v_a + \ldots + u \sum_{a,b} D_{ab} v_a v_b + \ldots \tag{3.30}$$

Following the discussion above, only the B_1, C_a , and D_{ab} terms contribute to the rate. One finds

$$\begin{aligned} C_a &= 2\,(2\kappa - \lambda_a)^{-1}\left\langle \overline{U}^2\overline{V}_a \right\rangle, \\ D_{ab} &= 3\,(2\kappa - \lambda_a - \lambda_b)^{-1}\left\langle \overline{U}^2\overline{V}_a\overline{V}_b \right\rangle, \\ B_1 &= -6T(2\kappa^{-1})\left((4\kappa)^{-1}\left\langle \overline{U}^4 \right\rangle + \sum_a (2\kappa - 2\lambda_a)^{-1}\left\langle \overline{U}^2\overline{V}_a^2 \right\rangle \right). \end{aligned} \tag{3.31}$$

The complete solution for ζ_1 is given in Appendix C. And the result for potentials with x^5 and x^6 terms is given in Appendix C.

Te form of ζ_1 suggests that we use modified propagators, or Green's functions[13]

$$\left(\omega_{ij} - c\delta_{ij}\right) G^{jk} = \delta_{ik} \implies G^{ij} = \sum_a \frac{\overline{V}_a^i \overline{V}_a^j}{\lambda_a - c}. \tag{3.32}$$

Here a excludes the negative eigenmode.

Before showing how ζ_1 affects the rate, note that including ζ_1 is the same as including operator insertions. To see this, pick one term from Equation 3.30, say $D_{ab} u v_a v_b$. When calculating the probability current, the factor of u disappears. And the remaining part is proportional to $v_a v_b = \overline{V}_a^i \overline{V}_b^j x^i x^j$. Adding this term to Equation 3.12, one could equally well have inserted an operator $\mathcal{O} \propto D_{ab} \overline{V}_a^i \overline{V}_b^j x^i x^j$. This operator can also receive loop corrections like in normal field theory.

The factorization into the statistical and dynamical prefactors rests on this vital fact: The dynamical prefactor only contains *single* operator insertions. In analogy with scattering theory, the dynamical prefactor contains connected diagram using external operators; the statistical prefactor is the sum of all vacuum diagram. The statistical prefactor expo-

13 This is expected from usual Feynman diagrams.

nentiates; the dynamical prefactor does not.

If one would like to push this program even further, additional corrections to ζ could be found by using $\zeta = \zeta_0 + \zeta_1\zeta_0' + \zeta_2\zeta_0' + \ldots$. Where $\zeta_n = \mathcal{O}(\lambda^n)$. In general, ζ_n is a polynomial of degree $4n-1$, and is completely determined by ζ_{n-1}. To wit for $n > 0$

$$T\partial_i^2\zeta_n + \partial_i\zeta_n\left[2\kappa u\overline{U}^i - \omega^{ij}x_j\right] + \kappa\zeta_n = \left(\kappa\frac{u}{T}\zeta_{n-1} + \partial_u\zeta_{n-1}\right)\left(\left\langle\overline{U}x^2\right\rangle + \left\langle\overline{U}x^3\right\rangle\right) + \sum_a \frac{\partial}{\partial v_a}\zeta_{n-1}\left(\left\langle\overline{V}^a x^2\right\rangle + \left\langle\overline{V}^a x^3\right\rangle\right) \tag{3.33}$$

Again, a does not include the negative eigenvalue κ.

Naively one would think that ζ_2 is sub-leading compared to ζ_1. Alas no. Indeed, look at c_a in Equation 3.30. We see that this term does not contribute directly to the rate. Instead this term contributes via the one-loop tadpole shown in Figure 1.

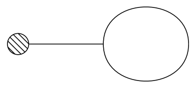

Figure 1: Tadpole contribution to the dynamical prefactor.

This tadpole insertion scales as λ_3^2, and similar terms exist in ζ_2. This is expected. Indeed, normally two cubic vertices are required for a non-vanishing result. As such, all $\sim \lambda_3^2$ terms in ζ_2 are relevant.

I here only note that the terms are of the form

$$\zeta_2 = uB' + uD'_{ab}v_a v_b + uF_{abcd}v_a v_b v_c v_c + \ldots \tag{3.34}$$

and leave the derivation for Appendix D. The explicit expressions are given in Equation D.3

In summary, the dynamical prefactor consists of operator insertions. And all of these multiply the full statistical prefactor.

3.4 Comparison With Known Results

Sections 3.2 and 3.3 derived the nucleation-rate for systems with n degrees of freedom. There are however pre-existing results for $n = 1$. Take a potential

$$V = -1/2\kappa x^2 + \frac{1}{3!}\lambda_3 x^3 + \frac{1}{4!}\lambda_4 x^4. \tag{3.35}$$

The NLO rate is [68, 76]:

$$\Gamma = \frac{\sqrt{|\kappa|}}{2\pi\eta}\left[1 - T\left(\frac{\lambda_4}{8\kappa^2} - \frac{5\lambda_3^2}{24\kappa^3}\right)\right]e^{-V_B/T}, \tag{3.36}$$

where as before the normalization from the metastable state is left implicit. This formula includes all corrections to the dynamical and statistical prefactors.

It is a encouraging that the statistical prefactor in Equation 3.23 together with the dynamical prefactor in Equation 3.31 (and ξ_2 from Equation D.3) reproduce Equation 3.36.

4 Generic Damping Coefficient

As yet all powder have been spent on the overdamped case. As such, let's now look at the generic-damping case. There are a few new features. First, the velocity, or rather the conjugate momenta, contribute to the Boltzmann factor. Second, the damping is not solely a multiplicative factor as in Equation 3.15. And third, the negative-eigenvalue direction contributes to the Boltzmann integral.

As before, the starting point is the Fokker-Planck equation [1, 71, 73]:

$$\frac{d}{dt}P = -\partial^i_x J^i_x - \partial^i_\pi J^i_\pi = \left[-\pi_i \partial^i_x + \partial^i_\pi\left[\eta \pi^i + \partial^i_x V\right] + \eta T \partial^i_\pi\right] P = 0, \tag{4.1}$$

here π^i are conjugate momenta of x^i, and η is the damping.

Because the derivation of the rate mirrors that given in Section 3, some steps are omitted.

Start by assuming

$$V(x + x_B) \approx V_B + \frac{1}{2} x_i \omega^{ij} x_j. \tag{4.2}$$

Next, make the ansatz $P = \zeta(\vec{x}, \vec{v}) P_0$ where $P_0 = e^{-E/T}$ and $E = \frac{1}{2}\pi_i^2 + V(x)$. Hence

$$\left[\pi^i \partial^i_x + \left[\eta \pi^i - \omega_{ij} x^j\right] \partial^i_\pi - \eta T \partial^2_\pi\right] \zeta = 0. \tag{4.3}$$

Using the ansatz $\zeta(\vec{x}, \vec{v}) = \zeta(u)$, where $u = \overline{U}^i_\pi \pi^i + \overline{U}^i_x x^i$, the equation becomes

$$\pi^i \overline{U}^i_x \zeta'(u) + \overline{U}^i_\pi\left[\eta \pi^i - \omega_{ij} x^j\right] \zeta'(u) - \eta T \overline{U}^2_\pi \zeta''(u) = 0. \tag{4.4}$$

For consistency

$$\pi^i \overline{U}^i_x + \overline{U}^i_\pi\left[\eta \pi^i - \omega_{ij} x^j\right] = -\lambda u = -\lambda\left[\overline{U}^i_\pi \pi^i + \overline{U}^i_x x^i\right]. \tag{4.5}$$

This implies that $\overline{U}^i_\pi$ is an eigenvector of ω_{ij}: $\overline{U}^i_\pi \omega_{ij} x^j = \kappa \overline{U}^i_\pi x^i$.

Whence

$$-\lambda \overline{U}^i_\pi = \left(\overline{U}^i_x + \eta \overline{U}^i_\pi\right) \ \ \& \ \ -\kappa \overline{U}^i_\pi = -\lambda \overline{U}^i_x, \tag{4.6}$$

so $\overline{U}_x$ is also an eigenvector of ω^{ij}.

Putting everything together one finds [1, 68]

$$\lambda = \frac{1}{2}\left(\pm\sqrt{\eta^2 - 4\kappa} - \eta\right). \tag{4.7}$$

Let's stop and make a few observations. First, we'll soon see that λ needs to be positive, so perforce $\kappa < 0$ and we must choose $\lambda = \frac{1}{2}\left(\sqrt{\eta^2 - 4\kappa} - \eta\right)$. Second, in the above solution $\overline{U}^i_\pi$ was a *single* eigenvector. One could instead take $\overline{U}^i_\pi$ as a linear combination of eigenvectors: $\overline{U}^i_\pi = \sum_a c_a \overline{V}^i$. This would however not work since each a would give a different λ.

All in all, we can choose $\overline{U}^i_x$ to be a normalized eigenvector of ω_{ij} and $\overline{U}^i_\pi = \frac{\lambda}{\kappa}\overline{U}^i_x$. Plugging everything into Equation 4.3 gives [1, 68]

$$\begin{aligned} &\gamma\zeta''(u) + u\zeta'(u) = 0, \\ &\gamma = \eta T \frac{\lambda}{\kappa^2} > 0. \end{aligned} \tag{4.8}$$

The solution satisfying the boundary conditions is

$$\zeta(u) = \frac{1}{\sqrt{2\pi\gamma}} \int_u^\infty e^{-\frac{u'^2}{2\gamma}} du' \tag{4.9}$$

Given $\zeta(u)$, it's straightforward to calculate the rate. Explicitly [1, 68]

$$\Gamma = \frac{\overline{U}^2_\pi \eta}{\sqrt{2\pi\gamma}} \int_{u=0} d^n x d^n \pi e^{-E/T}, \tag{4.10}$$

where $E = \frac{1}{2}\pi_i^2 + V(x)$.[14]

Doing the Gaussian integrals one finds up to a normalization

$$\Gamma = \frac{\lambda}{2\pi} \left|\det{}'\omega\right|^{-1/2} e^{-V_B/T}. \tag{4.11}$$

As before there are two types of contributions from higher orders. First from corrections to ζ, and second, higher-order corrections to E in the integral $\int_{u=0} d^n x d^n v e^{-E/T}$.

Before calculating these corrections, note that the rate is still real. The reason is however not the same as in Equation 3.13. Indeed, there the rate was real because $u = 0$ removed any fluctuations in the negative-eigenvalue direction. This is no longer the case. Instead, the rate is real because the conjugate momentum term overpowers the negative term in the potential.

To confirm this, denote the negative-eigenvalue direction by $x_u \equiv \overline{U}^i_x x^i$. The problematic term in the energy is

$$E = -\frac{1}{2}|\kappa| x_u^2 + \ldots \tag{4.12}$$

Now, if the rate is calculated at $u = 0$, the conjugate momenta corresponding to x_u, effectively changes κ. That is, at $u = 0$ we have $\pi_u = \overline{U}^i_\pi \pi^i = \frac{|\kappa|}{\lambda} x_u$. Hence

$$-|\kappa| \to \frac{\kappa^2}{\lambda^2} - |\kappa| = \frac{1}{2}\eta\left(\sqrt{\eta^2 + 4|\kappa|^2} + \eta\right) \equiv \overline{\kappa} > 0. \tag{4.13}$$

So all Gaussian integrals converge, and the rate is real.

14 One could also calculate the rate at $\overline{U}_x x^i = 0$ as is done in [1]. However, in that case great care must be taken since $\zeta(u)$'s contribution is non-trivial.

The rate is calculated at $u = 0$ (equivalently at $\overline{U}^i_x x^i = \frac{\lambda}{|\kappa|}\overline{U}^i_x \pi^i$), which seems rather mysterious at first. So let's see what this means. To avoid clutter I use $x_u \equiv \overline{U}^i_x x^i$ and $\pi_u \equiv \overline{U}^i_\pi \pi^i$. That is, x_u and π_u are position and conjugate momenta in the negative-eigenvalue direction. Denote the energy in this direction by $E_u \equiv \frac{1}{2}\pi_u^2 + \frac{1}{2}\kappa x_u^2$. At the saddle point $E_u = 0$. Consider now the motion of a particle starting at the saddle point. To do so, recall the static Fokker-Planck Equation:

$$\left[\pi_i \partial^i_x - \partial^i_\pi\left[\eta\pi^i + \partial^i_x V\right] - \eta T \partial^i_\pi\right] P = 0. \tag{4.14}$$

In addition, if $P = \zeta(\vec{x}, \vec{\pi})e^{-E/T}$, the Equation for $\zeta(\vec{x}, \vec{\pi})$ is

$$\left[\pi^i \partial^i_x + \left[\eta\pi^i - \partial^i_x V\right]\partial^i_\pi - \eta T \partial^2_\pi\right]\zeta = 0. \tag{4.15}$$

Namely, deviations from thermal equilibrium follow Equation 4.15, which is known as the adjoint, or backward (time-reversed), Fokker-Planck Equation.

Now, the Fokker-Planck Equation corresponds to a particle obeying

$$\dot{\pi}^i = -\eta\pi^i - \partial^i_x V + f(t), \tag{4.16}$$

the last term represents thermal noise and vanishes on average.

Likewise, the backward Fokker-Planck Equation follows from

$$\dot{\pi}^i = \eta\pi^i - \partial^i_x V + f(t), \tag{4.17}$$

Imagine now releasing a particle close to $x_u = \pi_u = 0$. If the particle evolves according to Equation 4.16, an unstable solution is [1]

$$x^i = x_0 e^{\lambda t} \quad \pi^i = x_0 \lambda e^{\lambda t}. \tag{4.18}$$

On this solution the energy is

$$E_u = -\frac{1}{2}\eta\lambda x_0^2 e^{2t\lambda}. \tag{4.19}$$

So the damping causes the energy to dissipate as expected: $\frac{d}{dt}E = -\eta v^2$.

Next, consider instead a particle following Equation 4.17. The unstable solution is now

$$x^i = x_0 e^{\frac{|\kappa|}{\lambda}t} \quad \pi^i = x_0 \frac{|\kappa|}{\lambda} e^{\frac{|\kappa|}{\lambda}t}, \tag{4.20}$$

with associated energy

$$E_u = \frac{1}{2}\eta\frac{|\kappa|}{\lambda}x_0^2 e^{2\frac{|\kappa|}{\lambda}t}. \tag{4.21}$$

This is precisely the solution implied by $u = 0$: $\pi_u = \frac{|\kappa|}{\lambda}x_u$. And so $u = 0$ simply denotes all particles connected to the saddle-point via Equation 4.17. Note that the energy in Equation 4.21 suppresses fluctuations away from the saddle point via the Boltzmann factor. This is why the integral is localized at $x_u = 0$ for $\eta \to \infty$.

Equation 4.21 also highlights a problem for small damping. Namely, for $\eta = 0$ the energy in Equation 4.21 identically vanishes. Effectively the negative-eigenmode turns into a zero-mode. While the rate is finite in the $\eta \to 0$ limit to leading order, it's doubtful that this generalizes to higher orders.

There are other indications that the formalism breaks down for small damping [68], and one should be cautious when using existing formulas [23, 64] for an underdamped system.

4.2 The Statistical Prefactor

Let's now include corrections to the statistical prefactor. The steps are mirror those of Section 3.2.

Start with the integral

$$Z[\overline{U}_x, \overline{U}_\pi] = \int d^n x d^n \pi e^{iku - 1/T \frac{1}{2}\left(\pi^i \pi^i + x_i \omega^{ij} x_j\right)}, \tag{4.22}$$

where $u = \overline{U}^i_x x^i + \overline{U}^i_\pi \pi^i$. This integral is equivalent to 4.10 after integrating over k.

One finds

$$Z[\overline{U}_x, \overline{U}_\pi] = \left[\det'|\omega|/(2\pi)\right]^{-1/2} (2\pi)^{-n/2} \exp\left[\frac{1}{2} k^2 T \left(\overline{U}^2_\pi + \overline{U}^i_x \omega^{-1}_{ij} \overline{U}^j_x\right)\right]. \tag{4.23}$$

We see that $Z[\overline{U}_x, \overline{U}_\pi]$ is a generating function, and the rule is

$$x^i \to k^{-1} \frac{\partial}{\partial \overline{U}^i_x} Z[\overline{U}_x, \overline{U}_\pi], \quad \pi^i \to k^{-1} \frac{\partial}{\partial \overline{U}^i_\pi} Z[\overline{U}_x, \overline{U}_\pi]. \tag{4.24}$$

The integral converges because

$$-T\left(\overline{U}^2_\pi + \overline{U}^i_x \omega^{-1}_{ij} \overline{U}^j_x\right) = \frac{T \eta \lambda}{\kappa^2} = \gamma > 0, \tag{4.25}$$

with γ given in Equation 4.8.

As before, consider the potential

$$V(x + x_B) = V_B + \frac{1}{2} x^i \omega^{ij} x^j + \frac{1}{4!} \lambda^{ijkl}_4 x^i x^j x^k x^l. \tag{4.26}$$

The Feynman rules are

$$\underline{\qquad\qquad\qquad} = \omega^{-1}_{ij}$$

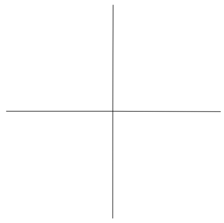 $= -\lambda_4^{ijkl}$

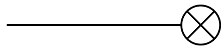 $= \delta^{ij}\kappa^{-1}\overline{U}^j_x$

In addition, of there're $2n$ external-current insertions, the diagram picks up a factor $(-1)^n\gamma^{-n}(2n-1)!!$; diagrams with an odd number of current insertions vanish.

Similarly, for integrals over conjugate momenta, the external current gives a factor $\delta^{ij}\overline{U}^j_\pi = \frac{\lambda}{\kappa}\delta^{ij}\overline{U}^j_x$, and the $2n$ rule is the same.

The derivation of the dynamical prefactor mirrors that of Section 3.3. Albeit messier. The details are given in Appendix B.

5 Field Theory

As yet I have not considered field theory, however, the field theory limit is straightforward [71]. Consider the overdamped case. Looking at Section 3, we see that these fields live in three dimensions. This is no accident. Indeed, there's a beautiful connection between thermal escape and dimensional reduction [4, 61].

In short this three-dimensional field theory arises from integrating out high-energy modes. As such, all mass parameters have thermal contributions, and couplings depend on the temperature.

Yet for the purposes of this paper we can ignore the details of dimensional reduction [48, 49], and three-dimensional parameters are taken as free. I will however absorb temperature factors in couplings and fields. In addition, I omit details associated with the assumed, effective, Langevin description. Uncertainties associated with this effective theory are important [4–7, 12–14], but are beyond the scope of this paper.

To see how things work, consider a real-scalar model with three-dimensional action

$$S_{\text{LO}}[\phi] = \int d^3x \left[\frac{1}{2}(\vec{\nabla}\phi)^2 + V(\phi)\right]. \tag{5.1}$$

The barrier position $\vec{x}_B$ is replaced with the bounce [23, 26]

$$\partial^2\phi_b(x) = V'(\phi_b), \quad \partial\phi_b|_{x=0} = 0, \quad \lim_{x\to\infty}\phi_b = \phi_S, \tag{5.2}$$

where ϕ_S denotes the metastable minima.

The action evaluated on the bounce is analogous to the barrier height:

$$V_B \to S_{\text{LO}}[\phi_b] \equiv S_B. \tag{5.3}$$

As for the potential, in Section 3 we assumed

$$V(x+x_B) = V_B + \frac{1}{2}x_i\omega^{ij}x_j + \frac{1}{3!}\lambda_3^{ijk}x^ix^jx^k + \frac{1}{4!}\lambda_4^{ijkl}x^ix^jx^kx^l. \tag{5.4}$$

In field theory this potential is replaced with (to forth order)

$$S_{\text{LO}}[\phi_b+\phi] = S_{\text{LO}}[\phi_b] + \frac{1}{2}\int d^3yd^3w\phi(y)\delta_y\delta_w S_{\text{LO}}[\phi_b]\phi(w) \tag{5.5}$$

$$+\frac{1}{3!}\int d^3yd^3wd^3z\delta_y\delta_w\delta_z S_{\text{LO}}[\phi_b]\phi(y)\phi(w)\phi(z) \tag{5.6}$$

$$+\frac{1}{4!}\int d^3yd^3wd^3zd^3v\delta_y\delta_w\delta_z\delta_v S_{\text{LO}}[\phi_b]\phi(y)\phi(w)\phi(z)\phi(v), \tag{5.7}$$

where δ_y is shorthand for $\frac{\delta}{\delta\phi(y)}$. The reason for writing everything in excruciating detail is that we can readily identify terms.

The dictionary is

$$x^i\omega^{ij}x^j \to \int d^3x\phi(x)\left[-\partial^2 + V''[\phi_b]\right]\phi(x) \tag{5.8}$$

$$\lambda_3^{ijk}x^ix^jx^k \to \int d^3xV'''[\phi_b]\phi(x)^3, \tag{5.9}$$

$$\lambda_4^{ijkl}x^ix^jx^kx^l \to \int d^3xV''''[\phi_b]\phi(x)^4. \tag{5.10}$$

Furthermore, the solution to the Fokker-Planck equation

$$P = \zeta(u)e^{-V/T}, \tag{5.11}$$

becomes [71] $P = \zeta(u)e^{-S_{\text{LO}}[\phi+\phi_b]}$ with $u = \int \overline{U}(x)\phi(x)$. The negative eigenvalue is

$$\left[-\partial^2 + V''[\phi_b]\right]\overline{U}(x) = \kappa\overline{U}(x), \quad \kappa < 0. \tag{5.12}$$

And analogous to Section 3

$$\zeta(u) = \frac{1}{\sqrt{2\pi|\alpha|}}\int_u^\infty du' e^{-u'^2/(2|\alpha|)}, \tag{5.13}$$
$$\alpha = \frac{1}{\kappa}.$$

5.1 Feynman Rules for the Statistical Prefactor

Consider the potential

$$V(\phi) = \frac{1}{2}m^2\phi^2 - \frac{1}{3!}g\phi^3 + \frac{1}{4!}\lambda\phi^4. \tag{5.14}$$

Expanding around the bounce gives[15]

$$\begin{aligned} V(\phi_b+\phi) =& V(\phi_b)+\frac{1}{2!}\phi^2\left[m^2-g\phi_b+\frac{1}{2}\lambda\phi_b^2\right] \\ &+\frac{1}{3!}\left[\lambda\phi_b-g\right]\phi^3+\frac{1}{4!}\lambda\phi^4. \end{aligned} \tag{5.15}$$

Using the result in Section 3.2, the Feynman rules are

 $= \Delta(x-y)$ 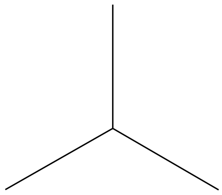 $= -(\lambda\phi_b(x)-g)$

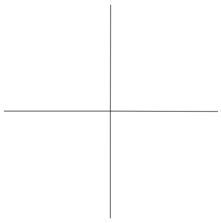 $= -\lambda$ 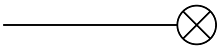 $= \kappa^{-1}\overline{U}(x),$

The propagator is defined by $\left[-\partial^2+V''[\phi_b(x)]\right]\Delta(x-y)=\delta^3(x-y)$; all zero eigenvalues are projected out as explained in Section 5.2. Also, this propagator depends on bounce, and needs to be found numerically, see Section 6.1 for the details.

The Feynman rules work as usual, with the new rule that if there are $2n$ external-current insertions, the diagram picks up an additional factor $(-1)^n\kappa^n(2n-1)!!$, and diagrams with an odd number of current insertions vanish.

As an example, consider the diagram

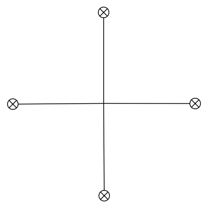

Using the Feynman rules we find

$$(-\lambda)/4!\kappa^{-4}(-1)^2\kappa^2(4-1)!!\int d^3x\overline{U}^4(x)=-3/4!\lambda\kappa^{-2}\int d^3x\overline{U}^4(x). \tag{5.16}$$

The dynamical prefactor is calculated via operator insertions as explained in Section 3.3. These operators are

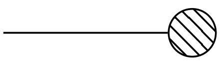 $= \sum_a \overline{V}_a(x)(\lambda_a-2\kappa)^{-1}\int d^3w\overline{U}^2(w)\overline{V}_a(w)(\lambda\phi_b(w)-g)$

15 I here ignore linear terms since the first-variation of the action vanishes.

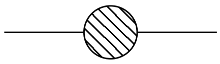 $$= \frac{1}{2}\lambda \sum_{ab} \overline{V}_a(x)\overline{V}_b(y)(\lambda_a+\lambda_b-2\kappa)^{-1}\int d^3w\overline{U}^2(w)\overline{V}_a(w)\overline{V}_b(w)$$

 $$= \lambda\frac{1}{4}\kappa^{-1}\int d^3x\left[(2\kappa)^{-1}\overline{U}^4(x)-\Delta_\kappa(x,x)\overline{U}^2(x)\right],$$

The first vertex acts as a tadpole, the second as a 2-point insertion, and the third is a number. Note that the second vertex can be reduced to a sum of propagators once it contracts. For example, because $\overline{V}_a(x)$ are eigenfunctions of the propagator, we have

$$\int d^3y\Delta(x,y)\overline{V}_a(y)=\overline{V}_a(x)\lambda_a^{-1}. \tag{5.17}$$

Then the leading correction involving the 2-point insertion is

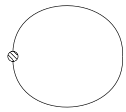

which after using the Feynman rules gives

$$\begin{aligned}&\frac{\lambda}{4}\sum_a \lambda_a^{-1}\frac{1}{\lambda_a-\kappa}\int d^3w\overline{U}^2(w)\overline{V}_a^2(w)=\\&\frac{\lambda}{4\kappa}\int d^3w\left[\Delta_\kappa(w,w)\overline{U}^2(w)-\Delta(w,w)\overline{U}^2(w)+\overline{U}^4(w)\kappa^{-1}\right]\end{aligned} \tag{5.18}$$

Amusingly the Δ_κ term cancels against the 0-point insertion at this order.

5.2 Zero-Modes

Consider now potential zero-modes. In field theory there are, at least, three zero-modes corresponding to the bounce [26, 66]. Naively these zero-modes invalidates the saddle-point approximation. Indeed, consider the statistical prefactor

$$A_{\text{stat}}=\int_{u=0}\mathcal{D}\phi e^{-S[\phi+\phi_b]}. \tag{5.19}$$

Since we are evaluating this integral via a saddle point approximation, there's a snag if any eigenvalue of $\delta^2S[\phi_b]$ vanishes. Concretely, expanding everything in an eigenbasis of $\delta^2S[\phi_b]$:

$$\begin{aligned}&S[\phi+\phi_b]=S_B+\frac{1}{2}\int d^3x\phi(x)\left[-\vec{\nabla}^2+V''[\phi_b(x)]\right]\phi(x)+\ldots\\&\phi(x)=\sum_a v_a\overline{V}_a(x)\\&\left[-\vec{\nabla}^2+V''[\phi_b(x)]\right]\overline{V}_a(x)=\lambda_a\overline{V}_a(x).\end{aligned} \tag{5.20}$$

The integral diverges if any $\lambda_a=0$ as there's no exponential suppression for large field values. These zero-modes are readily identified: $\overline{V}_\mu(x) = (S_B)^{-1/2}\,\partial_\mu\phi_b(x)$. The prefactor ensures that the eigenvectors are properly normalized [9, 11, 66].

Formally the problem can be solved by using collective coordinates [9, 11]

$$\phi(x) = \sum_a v_a \overline{V}_a(x - x_0). \tag{5.21}$$

where a excludes zero-modes. The integral over zero-modes is replaced by an integral over x_0. Essentially all zero-modes turn into a volume factor. And in particular, by using collective coordinates the zero-modes *never* appear in any propagator.

There is however a price to pay. Namely, projecting out the zero modes gives a Jacobean. To leading order this Jacobean is $(S_B)^{3/2}$(See Equation 2.4). If one does not venture to higher orders this is the end of the story, however, more care is needed at two loops and beyond.

Indeed, as pointed out in [9], there are additional terms coming from the Jacobean. To my knowledge the implications of these terms is unexplored. To see the effect of these terms, one can extend the result in [9] to 3-D field theory. And the result is

$$J_{ZM} = (S_B)^{3/2}\Big|1 + (S_B)^{-1}\int d^3x\,\phi(x)\partial^2\phi_b(x) \tag{5.22}$$

$$-(S_B)^{-2}\frac{1}{2}\int d^3x d^3y\,\phi(x)\phi(y)\left[\partial^2\phi_b(x)\partial^2\phi_b(y) + \partial_\mu\partial_\nu\phi_b(x)\partial_\mu\partial_\nu\phi_b(y)\right] \tag{5.23}$$

$$+(S_B)^{-3}A_3\Big|, \tag{5.24}$$

where[16]

$$A_3 = \int d^3x d^3y d^3z\,\phi(x)\phi(y)\phi(z)\Big[\frac{1}{3}\partial_\mu\partial_\nu\phi_b(x)\partial_\nu\partial_\alpha\phi_b(y)\partial_\alpha\partial_\mu\phi_b(z) - \frac{1}{2}\partial^2\phi_b(x)\partial_\mu\partial_\nu\phi_b(y)\partial_\mu\partial_\nu\phi_b(z) + \frac{1}{6}\partial^2\phi_b(x)\partial^2\phi_b(y)\partial^2\phi_b(z)\Big]. \tag{5.25}$$

The first term in J_{ZM} gives the familiar prefactor $(S_B)^{3/2}$. In this paper I don't include this prefactor explicitly as it cancels when calculating the statistical prefactor [47, 67].

The other terms are operator insertions that need to be taken into account order-by-order. Note that these zero-mode operators talk with the dynamical prefactor.

In summary, zero-modes don't appear in propagators, but there are operator insertions at higher orders. Also in models with Goldstone bosons there are equivalent Jacobeans corresponding to global symmetries [10].

5.3 Connection with the Effective Action

The rate is, in essence, an integral. An integral that needs to be calculated numerically for sure. But an integral nevertheless. It is however at times useful to view the rate as an

16 The second term in A_3 can be symmetrized over x, y and z.

effective action. Take for example the statistical prefactor

$$A_{\text{stat}} = \int_{u=0} \mathcal{D}\phi \, e^{-S[\phi+\phi_b]} = e^{-\overline{S}_{\text{eff}}[\phi_b]}. \tag{5.26}$$

The effective action is here a sum of all vacuum diagrams in the ϕ_b background. In getting to the right-hand side, we have a priori assumed that ϕ_b is a generic background field. To get to the actual rate one should in the end fix ϕ_b so that $\delta S_{\text{eff}}[\phi_b] = 0$. To leading order ϕ_b is just the tree-level bounce.

We could of course just calculate the integral in Equation 5.26 numerically, and brush-aside the effective action. For actual computations this is what one usually does. Yet the effective action has its uses. For example in cases with additional fields. If these fields are parametrically heavier than ϕ, they can be integrated out. In effect these fields generate, local, terms to the tree-level action for ϕ [75, 77, 78].

On the practical level the effective action let's one bypass tadpole diagrams. For example, diagrammatically the statistical prefactor in Equation 5.26 is (to two-loops)

The third diagram is not part of the effective action. Instead, corrections to the leading-order bounce incorporate all tadpoles. Explicitly, if the tree-level action is S_{LO} and the one-loop correction is S_{NLO}, then[17]

$$\delta S_{\text{LO}}[\phi_{\text{LO}}] = 0 \qquad \text{(The bounce solution)} \tag{5.27}$$

$$\phi_{\text{NLO}} \delta^2 S_{\text{LO}}[\phi_{\text{LO}}] + \delta S_{\text{NLO}}[\phi_{\text{LO}}] = 0 \qquad \text{(One-loop correction to the bounce)} \tag{5.28}$$

Including ϕ_{NLO} in the effective action gives

$$S_{\text{eff}}[\phi_b] = S_{\text{LO}}[\phi_b] + S_{\text{NLO}}[\phi_b] \tag{5.29}$$

$$\implies S_{\text{LO}}[\phi_{\text{LO}}] + \left[S_{\text{NLO}}[\phi_{\text{LO}}] - \frac{1}{2}\phi_{\text{NLO}}^2 \delta^2 S_{\text{LO}}[\phi_{\text{LO}}] \right] \tag{5.30}$$

Diagrammatically $S_{\text{NLO}}[\phi_{\text{LO}}]$ is the double-bubble, and $-\frac{1}{2}\phi_{\text{NLO}}^2 \delta^2 S_{\text{LO}}[\phi_{\text{LO}}]$ is the dumb-bell.

The actual expression for ϕ_{NLO} is given by

$$\phi_{\text{NLO}}(x) = -\int d^3y \, \Delta(x,y) \frac{\delta S_{\text{NLO}}[\phi_{\text{LO}}]}{\delta \phi(y)}. \tag{5.31}$$

This follows from the definition ϕ_{NLO}:

$$-\left[-\partial^2 + V''[\phi_{\text{LO}}(x)]\right] \phi_{\text{NLO}}(x) = \frac{\delta S_{\text{NLO}}[\phi_{\text{LO}}]}{\delta \phi(x)}. \tag{5.32}$$

Now, one need to be careful when using these formulas. Reason being that both the

17 I leave all integrals implicit.

propagator, and implicitly the effective action, are defined with zero-modes projected out. Concretely, if we expand

$$\phi_{\mathrm{NLO}}(x) = \sum_a v_a \overline{V}_a(x), \tag{5.33}$$

then

$$\left[-\partial^2 + V''[\phi_{\mathrm{LO}}(x)]\right] \phi_{\mathrm{NLO}}(x) = \sum_a \lambda_a v_a \overline{V}_a(x). \tag{5.34}$$

And only $\lambda_a \neq 0$ modes contribute—the bounce doesn't receive corrections in the zero-mode direction. What's more, no zero-modes appear in $\frac{\delta S_{\mathrm{NLO}}[\phi_{\mathrm{LO}}]}{\delta \phi(x)}$ since propagators are defined with zero-modes projected out. Furthermore, contributions in the negative-eigenvalue direction vanish for the same reason.

In summary, if the effective action is used, corrections to the leading-order bounce are zero in the negative/zero eigenmode directions. This makes calculations straightforward because neither imaginary nor divergent terms appear—normally coming from the negative and zero eigenmodes respectively.

5.4 Renormalization-Scale Invariance of the Rate

One of the most striking features in field theory is scale-independence. That is, calculations are independent of the renormalization scale. To show that the rate is scale-independent looks, at first, rather difficult. And to my knowledge this has never been explicitly demonstrated beyond one-loop. To that end, in this section I show analytically that the rate, dynamical prefactor included, is scale-independent to two loops.[18]

Why two loops? Well, in three dimensions explicit scale dependence shows up first at two loops. What's more, the two-loop beta function is the full beta function, and only the scalar mass parameter depends on the scale in three dimensions. For the model at hand the beta function is[19]

$$\frac{dm^2}{d\log\mu_3} = \frac{1}{16\pi^2}\frac{1}{3!}\lambda^2. \tag{5.35}$$

Before calculating the scale-dependence of the rate, it's instructive to first calculate the effective potential. That is, to treat $\phi_b \to \phi$ as a constant background field. This derivation parallels the nucleation-rate one.

The relevant diagram is

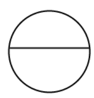

18 For models with radiative barriers renormalization-scale independence has been shown to NLO in [47, 57, 65].

19 I here ignore any tadpole corrections. And all the methods in this Section are readily extended to any model.

Using normal Feynman rules, the contribution to the effective potential is

$$-\frac{1}{3!\times 2!}(\lambda\phi-g)^2\int d^3xd^3y\Delta(x-y)^3=-\frac{1}{3!\times 2!}(\lambda\phi^2-g)\int d^3xd^3y\Delta(x)^3, \quad (5.36)$$

the last step only works if the background field is constant. The propagator in the background field is defined by

$$\left[-\partial^2+M^2\right]\Delta(x-y)=\delta^{(d)}(x-y), \qquad M^2\equiv V''(\phi). \quad (5.37)$$

The solution, in $d=3-2\epsilon$ dimensions, is [79]

$$\Delta(x)=\left(\frac{e^{\gamma}\mu_3^2}{4\pi}\right)^{\epsilon}\frac{1}{(2\pi)^{3/2-\epsilon}}\left(\frac{M}{|x|}\right)^{1/2-\epsilon}K_{1/2-\epsilon}(M|x|), \quad (5.38)$$

with K being the modified Bessel function. Note that for $\epsilon=0$ the propagator is

$$\Delta(x)=\frac{e^{-M|x|}}{4\pi|x|}. \quad (5.39)$$

Now, all ϵ poles, and associated scale-dependence, come from the $|x|\to 0$ region. While contributions from the $|x|\to\infty$ region are finite. The idea is to introduce a radial cut-off R, and for $|x|<R$ one should use the $d=3-2\epsilon$ expression for the propagator, while for $|x|\geq R$ one can directly take the $\epsilon\to 0$ limit [80]. Using properties of the Bessel function one finds

$$\int_{|x|<R} d^3x\Delta(x)^3=\frac{4\epsilon\log(\mu_3R)+(2+4\gamma)\epsilon+1}{64\pi^2\epsilon}. \quad (5.40)$$

The $\log R$ term cancels when including the region $|x|\geq R$ [80].

Here I just want to focus on the scale-dependent piece:

$$\frac{dV_{\text{2-Loop}}}{d\log\mu_3}=-\frac{1}{96\pi^2\times 2!}\lambda^3\phi^2, \quad (5.41)$$

which cancels with the running of the tree-level mass:

$$\frac{d}{d\log\mu_3}\left(\frac{1}{2}m^2\phi^2\right)=\frac{1}{16\pi^2}\frac{1}{2\times 3!}\lambda^2\phi^2. \quad (5.42)$$

With the effective-potential case done, most of the work carries over to the nucleation rate. First, note that the scale dependence of the leading-order action is[20]

$$\frac{d}{d\mu_3}S_{\text{LO}}[\phi_b]=\int d^3x\frac{1}{2}\phi_b^2\frac{d}{d\log\mu_3}m^2. \quad (5.43)$$

Second, as noted above, all scale-dependence comes from the $|x|\to 0$ region. The

20 $\frac{d}{d\log\mu_3}\phi_b$ terms cancel since the action is evaluated on-shell.

sunset diagram gives

$$-\frac{1}{3!\times 2!}\lambda^2\int d^3xd^3y\Delta(x,y)^3\phi_b(x)\phi_b(y). \tag{5.44}$$

To keep the discussion brief I here ignore terms linear in ϕ_b as they correspond to tadpoles.

The region of interest is $x\approx 0$. In this limit the propagator satisfies[21]

$$\begin{aligned}
&\left[-\partial^2+V''(\phi_b(x))\right]\Delta(x,y)=\delta^{(d)}(x-y)\\
&V''[\phi_b(x)]\approx V''[\phi_b(0)]+\ldots\\
&\implies\left[-\partial^2+V''[\phi_b(0)]\right]\Delta(x,x+y)=\delta^{(d)}(y)+\ldots
\end{aligned}\tag{5.45}$$

Thus to leading order this propagator is the same as for the effective-potential case [77]. Going back to the integral we find

$$-\frac{1}{3!\times 2!}\lambda^2\int d^3xd^3y\Delta(x,y)^3\phi_b(x)\phi_b(y)\approx-\frac{1}{3!\times 2!}\lambda^2\int d^3x\phi_b(x)^2\int_{|y|<R}d^3y\Delta(y)+\ldots$$

The integral over y is the same as before. All in all

$$\frac{d}{d\log\mu_3}S_{\text{2-Loop}}=-\frac{1}{96\pi^2\times 2!}\lambda^2\int d^3x\phi_b(x)^2. \tag{5.46}$$

So the effective action is RG-invariant as promised.

Next, let's check that the dynamical prefactor is RG-invariant. Up to a factor of 2π the RG dependence is[22]

$$\frac{d}{d\log\mu_3}\sqrt{|\kappa|}=-\frac{1}{2\sqrt{|\kappa|}}\int d^3x\overline{U}(x)^2\frac{d}{d\log\mu_3}m^2=-\frac{1}{96\pi^2\times 2!\sqrt{|\kappa|}}\lambda^2\int d^3x\overline{U}(x)^2$$

and the relevant 2-loop diagram is

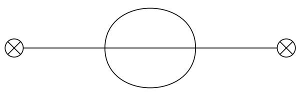

Using the Feynman rules from Section 5.1 this diagram is[23]

$$-\frac{1}{3!\times 2!}\kappa^{-1}\lambda^2\int d^3xd^3y\overline{U}(x)\overline{U}(y)\Delta(x,y)^3. \tag{5.47}$$

Using the same arguments as for the effective action we identify the scale-dependent

21 If one is uncomfortable with the derivative expansion, the same result follows after explicitly calculating the propagator. See Section 6.1.

22 This follows from the definition of the negative eigenvalue: $\left[-\partial^2+V''[\phi_b]\right]\overline{U}=\kappa\overline{U}$. Also, the RG-dependence we are calculating is technically at the three-loop level.

23 The minus sign comes from the $\overline{U}^n$ rule. Note also the sign of κ compared to $|\kappa|$.

piece

$$-\frac{d}{d\log\mu_3}\left\langle \lambda^2\kappa^{-1}\frac{1}{3!\times 2!}\int d^3x d^3y \overline{U}(x)\overline{U}(y)\Delta(x,y)^3\right\rangle = -\frac{1}{96\pi^2\times 2!\kappa}\lambda^2\int d^3x\overline{U}(x)^2.$$

The dynamical prefactor is manifestly RG-invariant once we multiply the above diagram with the leading-order prefactor $\frac{\sqrt{|\kappa|}}{2\pi}$.

Although this section only treated the real-scalar model, everything carries through once vector-bosons are included. The same methods can also be used to check that the Sphaleron rate is renormalization-scale invariant.

5.5 Radiative Barriers and the Dynamical Prefactor

The previous section dealt with scale-dependence arising from two-loop diagrams. Here, instead, I investigate what happens when heavy fields are integrated out. For example vector bosons. The procedure of integrating out particles, and consistently calculating the rate, has been studied in [9, 47, 61, 77, 78].

This scenario is relevant for radiative barriers, as even if a barrier is absent at tree-level, it can be generated from loops [62, 75]. The Standard Model (with a small Higgs mass) is a famous example with vector-bosons generating a barrier. In practice vector-bosons can be integrated out before the thermal escape occurs for the scalar field. Integrating out short-distance modes yield a number of terms. Some that are scale dependent.

As an example, consider an SU(2) gauge theory with a scalar in the fundamental, the leading-order potential is

$$V(\phi) = \frac{1}{2}m^2\phi^2 - \frac{1}{16\pi}e^3\phi^3 + \frac{1}{4}\lambda\phi^4. \tag{5.48}$$

The next order includes a contribution [47][24]

$$V_{\text{NLO}} \sim \frac{1}{1024\pi^2}e^4\int d^3x\phi^2(x)\left\{51\log\left(\frac{\mu_3^2}{\phi^2(x)e^2}\right) - 126\log(3/2) + 33\right\}. \tag{5.49}$$

Normally the scale dependence in V_{NLO} cancels with the running mass:

$$\frac{d}{d\log\mu_3}m^2 = -\frac{51}{256\pi^2}e^4 + \dots \tag{5.50}$$

This is manifestly the case for the statistical prefactor, but it's more complicated for the dynamical prefactor. Indeed, naively the negative eigenvalue satisfies

$$\left[-\nabla^2 + V''[\phi_b]\right]\overline{U} = \kappa\overline{U}, \tag{5.51}$$

which implies

$$\delta\kappa = \int d^3x V''_{\text{NLO}}[\phi_b(x)]\overline{U}(x)^2. \tag{5.52}$$

24 I here ignore terms that don't affect scale-dependence at this order.

Let's check that this procedure is correct by using the methods in Section 3.3. Treating V_{NLO} as a perturbation, the scale-dependent piece in ζ_1 is (see Equation 3.26)

$$\delta\zeta_1 = (2\kappa)^{-1}\frac{51}{256\pi^2}e^4 u\log\mu_3. \tag{5.53}$$

So the contribution to the rate is $\delta\Gamma = \frac{\sqrt{|\kappa|}}{\sqrt{2\pi}}(2\kappa)^{-1}\left[\frac{51}{256\pi^2}e^4\log\mu_3\right]e^{-\bar{S}_{\text{eff}}}$.

As shown above, the RG-dependence of κ is $\frac{d}{d\log\mu_3}\kappa = \frac{51}{256\pi^2}e^4$. This in turn implies a scale-dependence for the dynamical prefactor:

$$\delta A_{\text{dyn}} = -\frac{\sqrt{|\kappa|}}{\sqrt{2\pi}}(2\kappa)^{-1}\frac{51}{256\pi^2}e^4. \tag{5.54}$$

Using the contribution from $\delta\zeta_1$, we see that the dynamical prefactor is RG-invariant.

5.6 Factorization of the Rate

In the previous Sections I have shown that the rate factorize as

$$\Gamma = A_{\text{dyn}} \times A_{\text{stat}}. \tag{5.55}$$

The Statistical prefactor is

$$A_{\text{stat}} = \int_{u=0} \mathcal{D}\phi\, e^{-S[\phi+\phi_b]} \times J_{ZM} \equiv e^{-\bar{S}_{\text{eff}}[\phi_b]}. \tag{5.56}$$

Here $\bar{S}_{\text{eff}}[\phi_b]$ omits all contributions from negative eigenmodes and zero-mode. The zero modes also generate operator insertions; these are included in J_{ZM} as discussed in Section 5.2. For concrete calculations, the Feynman rules given in Section 5.1 can be used.

The entire rate should be normalized with $e^{-\int d^3x V_{\text{eff}}(\phi_S)}$, where $V_{\text{eff}}(\phi_S)$ denotes the effective potential in the metastable state.[25]

The dynamical prefactor is defined as

$$A_{\text{dyn}} = \frac{1}{\eta \times A_{\text{stat}}}\int_{u=0}\mathcal{D}\phi\left[\int d^3x\bar{U}(x)\delta_{\phi(x)}\zeta(\phi)\right]e^{-S[\phi+\phi_b]} \times J_{ZM}. \tag{5.57}$$

Or equivalently, I define A_{dyn} as all terms in the rate that don't exponentiate—barring zero-mode contributions. So A_{dyn} is the sum of all connected diagrams involving operator-insertions given by $\zeta(\phi)$.

The virtue of these definitions is that the renormalization-scale dependence for A_{dyn} and A_{stat} are simple; both A_{stat} and A_{dyn} are manifestly real to all orders; A_{dyn} and A_{stat} can be calculated independently; there is a clear physical interpretation with A_{stat} as the Boltzmann suppression, and A_{dyn} as the probability-flow across the saddle-point.

To leading order A_{dyn} can be interpreted as the growth-rate of the bubble—this is not true to higher-orders.

25 This last point is important since A_{stat} is not finite without the normalization. In practice $V_{\text{eff}}(\phi_S)$ should be included diagram-by-diagram as discussed in Section 6.2.

6 Considerations for Concrete Calculations

In the previous section I derived the rate, at higher orders, and performed sundry cross-checks. However, for actual calculations there are several subtleties that appear. To that end, this section shows how to calculate propagators in an inhomogeneous bounce background; what diagrams appears beyond the functional determinant; and how to isolate divergences in dimensional regularization.

6.1 Green's Functions

To calculate Feynman diagrams one invariably deals with propagators, or equivalently Green's functions. Yet these are more tricky in the bounce background:

$$\left[-\partial^2 + V''[\phi_b(x)]\right]\Delta(x,y) = \delta^3(x-y). \tag{6.1}$$

It is clear that little can be done without numerics. Indeed, often not even the bounce is known analytically, and even if it were, finding $\Delta(x,y)$ would be unpleasant.

Because the bounce is spherically symmetric, it's useful to expand the propagator in spherical harmonics [81]

$$\Delta(x,y) = \frac{1}{4\pi}\sum_{l=0}^{\infty}(2l+1)P_l(\cos\alpha)\Delta_l(r,r'), \tag{6.2}$$

with the short-hand $r \equiv |\vec{x}|$, $r' \equiv |\vec{y}|$ and $\cos\alpha = \frac{\vec{x}\cdot\vec{y}}{|\vec{x}||\vec{y}|}$.

Here $\Delta_l(r,r')$ satisfies

$$\left[-\partial_r^2 - \frac{2}{r}\partial_r + \frac{l(l+1)}{r^2} + V''[\phi_b(r)]\right]\Delta_l(r,r') = -\delta(r-r')/r^2. \tag{6.3}$$

First the bounce needs to be found numerically. Equation 6.3 can then by solved numerically for given l.

There are two caveats. For practical reasons one can't solve Equation 6.3 for infinitely many l. Also, the propagator diverges in the $\vec{x}\to\vec{y}$ limit.

Both of these problems have a common solution. The idea is to solve Equation 6.3 for $l \in (1,L)$ for some L, typically between 50 to 100.[26] Then, the remaining part of the l sum can be done analytically. This large l region is responsible for divergent terms.

There are two cases. First, assume that $\cos\alpha < 1$. Solving Equation 6.3 (see Appendix E) for large l one finds

$$\frac{1}{4\pi}\sum_{l=L+1}^{\infty}(2l+1)P_l(\cos\alpha)\Delta_l(r,r') = \delta_L + \frac{1}{4\pi}\frac{1}{|\vec{x}-\vec{y}|}, \tag{6.4}$$

$$\delta_L = -\frac{1}{4\pi}\sum_{l=0}^{L}(2l+1)\Delta_l(r,r')P_l(\cos\alpha). \tag{6.5}$$

26 The precise value for L can be found adaptably by demanding that the numerical solution and the approximate one in Equation E.6 agrees to, say, 1%.

The δ_l term can be evaluated numerically for given L.

For the second case we assume $\cos\alpha = 1$, and find

$$\frac{1}{4\pi}\sum_{l=L+1}^{\infty}(2l+1)P_l(1)\Delta_l(r,r') = \delta_L + \frac{1}{4\pi}\frac{\Gamma(1-2\epsilon)}{\Gamma(1-\epsilon)}\left(\mu^2 e^{\gamma}\right)^{\epsilon}(||x|-|y||)^{2\epsilon-1} \tag{6.6}$$

$$\delta_L = \begin{cases} -\frac{1-(|y|/|x|)^{L+1}}{4\pi(|x|-|y|)} & \text{if } |x|>|y| \\ -\frac{1-(|x|/|y|)^{L+1}}{4\pi(|y|-|x|)} & \text{if } |x|<|y| \end{cases} \tag{6.7}$$

Note that the δ_L term is finite in the $|x|\to|y|$ limit. Also, above I only included the leading terms. Higher-order terms are given in Appendix E.

That leaves zero modes. Luckily these only contribute to $l=1$. To remove the zero-modes, start with Equation 6.1

$$\left[-\partial^2 + V''[\phi_b(x)]\right]\Delta(x,y) = \delta^3(x-y). \tag{6.8}$$

Now use the representation

$$\Delta(x,y) = \sum_a \frac{\overline{V}_a(x)\overline{V}_a(y)}{\lambda_a}, \tag{6.9}$$

where $\overline{V}_a(x)$ is an eigenfunction of $\left[-\partial^2 + V''[\phi_b(x)]\right]$ with eigenvalue λ_a. From Section 5.2 we know that the, normalized, zero-modes are [9, 10]

$$\overline{V}_\mu = (S_B)^{-1/2}\partial_\mu\phi_b. \tag{6.10}$$

So if we instead consider the equation

$$\left[-\partial^2 + V''[\phi_b(x)] + \epsilon\right]\Delta^{\epsilon}(x,y) = \delta^3(x-y), \tag{6.11}$$

we can remove the zero eigenvalues by defining

$$\Delta'(x,y) = \lim_{\epsilon\to 0}\left[\Delta^{\epsilon}(x,y) - (S_B)^{-1}\sum_\mu \frac{\partial_\mu\phi_b(x)\partial_\mu\phi_b(y)}{\epsilon}\right]. \tag{6.12}$$

This modified propagator, also known as a Generalized Green's function, satisfies

$$\left[-\partial^2 + V''[\phi_b(x)]\right]\Delta'(x,y) = \delta^3(x-y) - (S_B)^{-1}\partial_\mu\phi_b(x)\partial_\mu\phi_b(y). \tag{6.13}$$

The above equation can be solved by expanding in spherical harmonics. And as mentioned, the $\partial_\mu\phi_b(x)\partial_\mu\phi_b(y)$ term only contributes to $l=1$.

In summary:

1. Solve the bounce equation $\partial^2\phi_b(x) = V'(\phi_b)$ numerically
2. Use Equations 6.2 and 6.3 to solve the Green's function for $l = 0,\dots L$. Choose L according to the required precision.
3. Introduce an angular cut-off $\delta \ll 1$, and define $1-\alpha = \frac{\vec{x}\cdot\vec{y}}{|\vec{x}||\vec{y}|}$.

4 If $\alpha \geq \delta$, use Equation 6.4 to do the sum from $l = L+1$ to ∞.

5 If $\alpha < \delta$, use Equation 6.6 to do the sum from $l = L+1$ to ∞.

6 When calculating integrals of the form $\int d^3x d^3y \Delta(x,y)$, use the result from point 5 to analytically calculate the contribution from the $\vec{x} \to \vec{y}$ region.

7 All ϵ poles, with $d = 3-2\epsilon$, come from the $\vec{x} \to \vec{y}$ region.

8 Integrate over the remaining phase-space numerically.

In addition, external-current insertions can be avoided by replacing

$$\Delta(x,y) \to \Delta(x,y) - \frac{\overline{U}(x)\overline{U}(y)}{\kappa}. \tag{6.14}$$

6.2 Statistical Prefactor

Here I show all diagrams appearing at the two-loop level. In addition, the scaling of each diagram is given. For brevity I use the real-scalar model defined in Section 5 with a large damping.

Diagrams contributing to the statistical prefactor can be divided into three classes: Vacuum diagrams, external-current contributions, and zero-mode contributions. Note that at NLO—equivalent to two loops for equilibrium observables—there are contributions from lower-loop diagrams with operator-insertions.

The Feynman rules are the same as in Section 5.1, and κ denotes the negative eigenvalue, and $\overline{U}(x)$ is the corresponding eigenvector normalized as $\int d^3x \overline{U}(x)^2 = 1$. All propagators are defined with zero-modes removed.

6.2.1 Vacuum Diagrams

There are three vacuum diagrams at two loops. The double-bubble, the dumbbell, and the sunset. Note that the dumbbell can also be calculated via the effective action, see Section 5.3.

The bubble and sunset diagrams are only finite after normalizing with the effective potential (in the metastable state). So for actual calculations one should always add the corresponding diagram for the effective potential with a relative minus sign. For example, the double-bubble gives

$$\frac{1}{8}\lambda \int d^3x \Delta(x,x)^2. \tag{6.15}$$

The divergence comes from the $|x| \to \infty$ region. Essentially the bounce reaches the false vacuum and the bounce becomes constant. For numerical stability one should include the effective-potential term directly:

$$\frac{1}{8}\lambda\int d^3x\Delta(x,x)^2 \to \frac{1}{8}\lambda\int d^3x\left[\Delta(x,x)^2-\Delta_S(x,x)^2\right], \tag{6.16}$$

where $\Delta_S(x,x)$ is the propagator for a constant $\phi=\phi_S$.

Since all diagrams exponentiate I directly include them in the effective action. This gives an extra minus sign for each diagram. To estimate the size of each diagram I use the power-counting

$$\Delta(x,y)\sim m,\quad \phi_b^2\sim m^2\lambda^{-1},\quad d^3x\sim m^{-3},\quad m^2\sim\lambda\sim g^2,\quad \frac{m}{\lambda}\gg 1. \tag{6.17}$$

The leading-order action then scales as $S_{\text{LO}}\sim\frac{m}{\lambda}$. At NLO the relevant contributions scale as $\frac{\lambda}{m}$.

Now for the actual diagrams. The double-bubble gives

$$\frac{1}{8}\lambda\int d^3x\Delta(x,x)^2\sim\frac{\lambda}{m} \tag{6.18}$$

And the dumbbell diagram is

$$-\frac{1}{8}\int d^3xd^3y(\lambda\phi_b(x)-g)(\lambda\phi_b(y)-g)\Delta(x,x)\Delta(x,y)\Delta(y,y)\sim\frac{\lambda}{m}. \tag{6.19}$$

And finally for the sunset diagram

$$-\frac{1}{3!\times 2!}\int d^3xd^3y(\lambda\phi_b(x)-g)(\lambda\phi_b(y)-g)\Delta(x,y)^3\sim\frac{\lambda}{m}. \tag{6.20}$$

6.2.2 External-Current Insertions

Here I label the diagrams by the order they appear, left to right and top to bottom. All diagrams scale as $\frac{\lambda}{m}$. The diagrams are

$$D_1=-\frac{1}{4}\lambda\kappa^{-1}\int d^3x\Delta(x,x)\overline{U}(x)^2, \qquad D_2=3\frac{\lambda}{4!}\kappa^{-2}\int d^3x\overline{U}(x)^4,$$

$$D_3=\frac{1}{4}\kappa^{-1}\int d^3xd^3yA(x,y)\Delta(x,y)^2\overline{U}(x)\overline{U}(y), \qquad D_4=-\frac{3}{4!}\kappa^{-2}\int d^3xd^3yA(x,y)\Delta(x,y)\overline{U}(x)^2\overline{U}(y)^2,$$

$$D_5=\frac{15}{72}\kappa^{-3}\left(\int d^3x(\lambda\phi_b(x)-g)\overline{U}(x)^3\right)^2, \qquad D_6=\frac{1}{8}\kappa^{-1}\left(\int d^3x(\lambda\phi_b(x)-g)\Delta(x,x)\overline{U}(x)\right)^2,$$

$$D_7=\frac{3}{6}\kappa^{-2}\left(\int d^3x(\lambda\phi_b(x)-g)\overline{U}(x)^3\right)\left(\int d^3x(\lambda\phi_b(x)-g)\Delta(x,x)\overline{U}(x)\right).$$

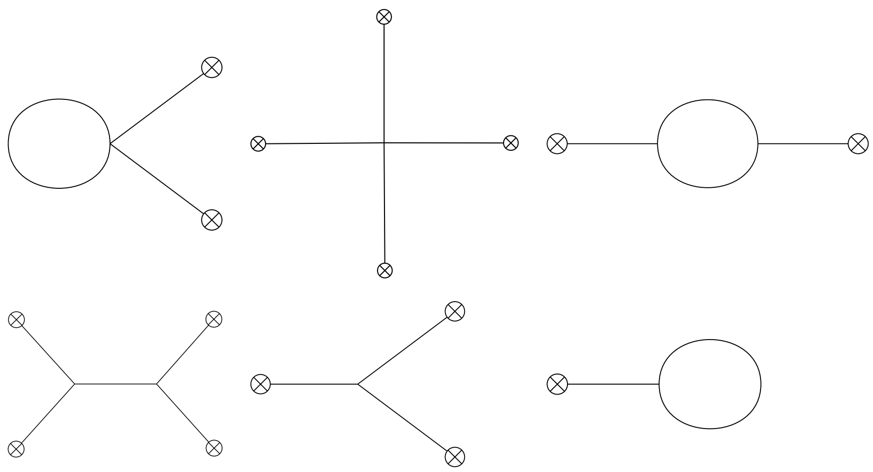

Here I use the shorthand $A(x,y) \equiv (\lambda\phi_b(x)-g)(\lambda\phi_b(y)-g)$. In the above, D_5 represents the square of diagram 5, D_6 the square of diagram 6, and D_7 the product of diagrams 5 and 6. Note that all diagrams are finite in the $|\vec{x}| \to \infty$ limit.

6.2.3 Zero-Mode Insertions

As noted in Section 5.2, when going to collective coordinates, there's a non-trivial Jacobean. This Jacobean is equivalent to operator insertions. These are given in Equation 5.22. I denote these operators with black circles to differentiate them from other operators. In addition, external-current insertions are not shown.

That said, the diagrams are

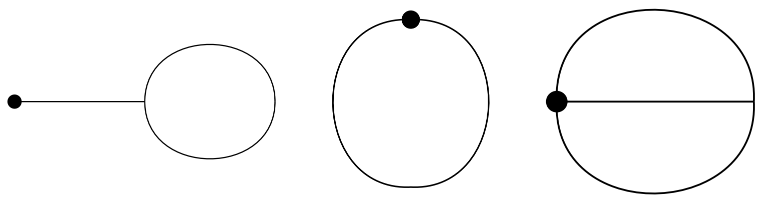

In terms of propagators these diagrams give

$$D_1 = \frac{1}{2}(S_{\text{LO}})^{-1}\int d^3xd^3y\partial^2\phi_b(x)\Delta(x,y)\Delta(y,y),$$
$$D_2 = -\frac{1}{2}(S_{\text{LO}})^{-2}\int d^3xd^3y\Delta(x,y)\left[\partial^2\phi_b(x)\partial^2\phi_b(y)-\partial_\mu\partial_\nu\phi_b(x)\partial_\mu\partial_\nu\phi_b(y)\right], \quad (6.21)$$
$$D_3 = -\frac{1}{3!}(S_{\text{LO}})^{-3}\int d^3xd^3yd^3zd^3w(\lambda\phi_b(x)-g)\Delta(x,w)\Delta(y,w)\Delta(z,w)\bar{A}(x,y,z),$$

where

$$\begin{aligned}\bar{A}(x,y,z) =& 2\partial_\mu\partial_\nu\phi_b(x)\partial_\nu\partial_\alpha\phi_b(y)\partial_\alpha\partial_\mu\phi_b(z)+\partial^2\phi_b(x)\partial^2\phi_b(y)\partial^2\phi_b(z)\\ &-\partial^2\phi_b(x)\partial_\mu\partial_\nu\phi_b(y)\partial_\mu\partial_\nu\phi_b(z)-\partial^2\phi_b(y)\partial_\mu\partial_\nu\phi_b(x)\partial_\mu\partial_\nu\phi_b(z)\\ &-\partial^2\phi_b(z)\partial_\mu\partial_\nu\phi_b(x)\partial_\mu\partial_\nu\phi_b(y).\end{aligned} \quad (6.22)$$

Note that $D_1 \sim D_2 \sim \frac{\lambda}{m}$, while $D_3 \sim \frac{\lambda^2}{m^2}$. So only D_1 and D_2 are relevant at NLO.

6.3 Dynamical Prefactor

The dynamical prefactor is given in Section 3.3. There are two types of contributions. Those coming from a quartic vertex and those coming from two cubic vertices.

The quartic contribution is given in Equation 5.18, and gives

$$\delta A_{\text{dyn}} = \frac{\lambda\sqrt{|\kappa|}}{2\pi\eta}\left[\frac{3}{8\kappa^2}\int d^3x\overline{U}(x)^4 - \frac{1}{4\kappa}\int d^3x\Delta(x,x)\overline{U}(x)^2\right]. \tag{6.23}$$

The double-cubic contribution has one part coming from Equation 3.31, and another from D.6. The contribution from Equation 3.31 give two diagrams

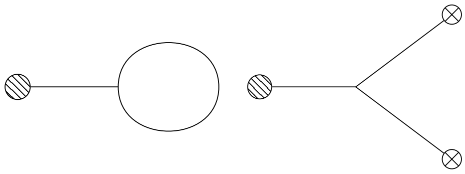

The first diagram is

$$-\frac{1}{4\kappa}\int d^3xd^3y\overline{U}(x)A(x,y)[\Delta_{2\kappa}(x,y)-\Delta(x,y)]\Delta(y,y)+\frac{1}{2}\kappa^{-2}\int d^3xd^3y\overline{U}(x)^3\overline{U}(y)\Delta(y,y)A(x,y),$$

and the second gives

$$\frac{1}{2}\kappa^{-2}\int d^3xd^3y\overline{U}(x)A(x,y)[\Delta_{2\kappa}(x,y)-\Delta(x,y)]\overline{U}(y)^2-\kappa^{-3}\int d^3xd^3y\overline{U}(x)^3\overline{U}(y)^3A(x,y).$$

6.3.1 Zero-Mode Insertions

As mentioned, the operators from the zero-mode Jacobian also talk with the dynamical prefactor. There are two one-loop diagrams (ignoring external-current insertions):

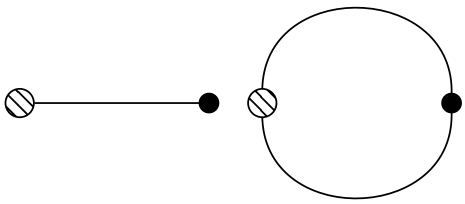

The first diagram gives

$$-\kappa^{-2}(S_B)^{-1}\int d^3x\int d^3y\partial^2\phi_b(y)(\lambda\phi_b(x)-g)\overline{U}(x)^2\left[\overline{U}(y)\overline{U}(x)-\frac{\kappa}{2}(\Delta_{2\kappa}(x,y)-\Delta(x,y))\right]\sim\frac{\lambda}{m}.$$

The second diagram is of order $\frac{\lambda^2}{m^2}$, and so is not relevant at this order.

7 Discussion

7.1 Summary

In this paper I have shown that the nucleation rate factorize into an equilibrium and non-equilibrium contribution—a statistical and dynamical prefactor. This factorization holds to all orders assuming an effective Langevin description. The formula derived in this paper lays the groundwork for calculating the nucleation rate beyond leading order—this is critical for getting a hold on uncertainties, and in particular, estimating when the formalism breaks down.

To ease calculations, this paper derives special Feynman rules. These are applied to several examples. In addition, explicit calculations confirm that both the dynamical and statistical prefactors are scale-invariant to two-loops—including scenarios with radiative barriers.

7.2 Future Work

Much work remains for robust descriptions of phase transitions. In particular, related to bubble-nucleation, this paper does not discuss gauge invariance of the dynamical prefactor. Even though the statistical prefactor is gauge invariant [57, 59, 60, 65], it's still important to verify the gauge independence of the full rate.

Another avenue is to apply the formalism of this paper to Sphaleron transitions. This is of great importance for Baryogenesis scenarios [43]. And in particular, the literature lacks a robust calculation of the Sphaleron rate with a radiative barrier. What's more, calculations of the functional determinant are limited to the Standard Model [82, 83].

Lastly, this paper is based on classical field theory. This is motivated at high temperatures. As integrating out high-energy modes results in a classical field theory with effective damping, couplings, and thermal noise. Explicit calculations of the damping are however sparse [4–8, 84]. And there are only a few calculations of the damping for realistic scenarios, gravitational-wave wise. Not to mention that calculating the damping to higher orders is required for precise predictions. There's also the question whether a Langevin description is applicable at higher orders. Answering these questions is part and parcel for robust predictions.

7.3 Conclusion

It is the hope that the results of this paper will aid the theoretical understanding of phase transitions, and thereby reduce uncertainties for gravitational-wave predictions. Yet there are several open questions, and sundry problems remain. Solving these problems requires applying existing methods to new models; pushing high-temperature field theory to higher orders; doing vital cross-checks with lattice computations; and connecting phase-transition calculations with gravitational-wave ones.

Acknowledgement

I would like to thank Oliver Gould, Joonas Hirvonen, and Johan Löfgren for discussions and a critical read-through of the manuscript. I am also indebted to Hamburg University and DESY for their hospitality. I am grateful to Aleksi Vuorinen and the Helsinki Institute of physics for their kind invitation to the University, where the final stages of this project took place. This work has been supported by the Swedish Research Council, project number VR:2021-00363. This work is supported by the Deutsche Forschungsgemeinschaft under Germany's Excellence Strategy - EXC 2121 Quantum Universe - 390833306.

A Different Damping Coefficients

So far I have assumed a single damping coefficient for all x^i. Yet everything works with multiple damping coefficients. Here I want to focus on a particular scenario relevant to Electroweak theory. As before consider the overdamping limit. Split the degrees of freedom into $x^i = (x_1^i, x_1^i)$. Here x_1^i have damping coefficient η_1, and x_2^i have η_2. Here I imagine that x_1^i plays the role of the Higgs field, and x_2^i that of the SU(2) gauge field.

The corresponding Fokker-Planck equation is

$$\partial_t P = \frac{1}{\eta_1}\left[\partial_i^1\left(P\partial_i^1 V\right) + T\partial_i^1\partial_i^1 P\right] + \frac{1}{\eta_2}\left[\partial_2^i\left(P\partial_i^2 V\right) + T\partial_2^i\partial_2^i P\right] \tag{A.1}$$

Following Section 3, make the ansatz $P = \zeta(u)e^{-V_B/T - x_i\omega^{ij}x_j/T}$, where $u = \overline{U}_1^i x_2^i + \overline{U}_2^i x_2^i$. This gives

$$T\left[\frac{\overline{U}_1^2}{\eta_1} + \frac{\overline{U}_2^2}{\eta_2}\right]\zeta''(u) - \left[\frac{1}{\eta_1}\overline{U}_1^i\omega_{ij}x^j + \frac{1}{\eta_2}\overline{U}_2^i\omega_{ij}x^j\right]\zeta'(u) = 0. \tag{A.2}$$

Consistency requires

$$\left[\frac{1}{\eta_1}\overline{U}_1^i\omega_{ij}x^j + \frac{1}{\eta_2}\overline{U}_2^i\omega_{ij}x^j\right] = -\alpha u, \tag{A.3}$$

for some $\alpha > 0$.

In the Standard Model the Higgs damping is parametrically smaller than the gauge field one, or, $\eta_2 \gg \eta_1$. So to leading order

$$\overline{U}_1^i\omega_{ij}x^j = -\eta_1\alpha\overline{U}_1^i x_1^i. \tag{A.4}$$

And $\overline{U}_1^i$ is the x_1^i part of the eigenvector with negative eigenvalue.

In the Standard Model for example the Higgs damping is $\eta_H \sim \alpha_w(\log 1/g)^{-1}$ [4,5,7,8], and the weak-gauge-boson damping is $\eta_L \sim (\log 1/g)^{-1} \gg \eta_H$.

B The Dynamical Prefactor for General Damping

Consider the potential

$$V(x+x_B)=V_B+\frac{1}{2}x_i\omega^{ij}x_j+\frac{1}{3!}\lambda_3^{ijk}x_ix_jx_k+\frac{1}{4!}\lambda_4^{ijkl}x_ix_jx_kx_l. \tag{B.1}$$

The goal is to solve Equation 4.3 and find ζ. That is, we need to solve

$$\left[\pi^i\partial_x^i+\left[\eta\pi^i-\partial_x^iV\right]\partial_\pi^i-\eta T\partial_\pi^2\right]\zeta=0. \tag{B.2}$$

The leading-order solution, refereed henceforth as ζ_0, is given in Equation 4.9.

Following Section 3.3, I make the ansatz $\zeta=\zeta_0+\zeta_1\zeta_0'(u)$. Plugging this ansatz into Equation B.2 one finds

$$-T\eta\partial_\pi^2\zeta_1+\left[\pi^i\partial_x^i+\eta\pi^i\partial_\pi^i-x^i\omega^{ij}\partial_\pi^j+2\eta T\frac{u}{\gamma}\overline{U}_\pi^i\partial_\pi^i\right]\zeta_1+\lambda\zeta_1=\left\langle\overline{U}_\pi x^2\right\rangle+\left\langle\overline{U}_\pi x^3\right\rangle, \tag{B.3}$$

where $\left\langle x^3\right\rangle\equiv\frac{1}{2!}\lambda_3^{ijk}x_ix_jx_k$, $\left\langle x^4\right\rangle\equiv\frac{1}{3!}\lambda_4^{ijkl}x_ix_jx_kx_l$, and $\overline{U}_\pi^i\overline{U}_\pi^i=\frac{\lambda^2}{\kappa^2}$.

As in Section 3.3 the idea is to use a polynomial ansatz for ζ_1, however, this ansatz is more involved than in the overdamping case. To see how things work, focus on the $\left\langle\overline{U}_\pi x^3\right\rangle$ term.

The idea is to use the eigenbasis ω: $\overline{V}_a^i\omega_{ij}=\lambda_a\overline{V}_a^j$. One can then expand $\pi^i=u_\pi\overline{U}_x^i+\sum_{a\neq\kappa}\overline{V}_a^i v_\pi^a$ and $x^i=u_x\overline{U}_x^i+\sum_{a\neq\kappa}\overline{V}_a^i v_x^a$.

The ansatz is

$$\begin{aligned}\zeta_1&=A+C_1u_x^2+C_1^au_xv_x^a+C_1^{ab}v_x^av_x^b\\&\quad+E_1u_\pi^2+E_1^au_\pi v_\pi^a+E_1^{ab}v_\pi^av_\pi^b\\&\quad+F_1u_\pi u_x+F_1^au_xv_\pi^a+F_2^au_\pi v_x^a+F_1^{ab}v_x^av_\pi^b.\end{aligned} \tag{B.4}$$

Solving Equation B.3, and keeping only terms that contribute to the rate, gives

$$E_1=\left\langle\overline{U}_x^3\right\rangle\frac{2}{-6\eta^2\kappa+27\kappa^2},\quad F_1=(-2\beta-\lambda)E_1,\quad C_1=\frac{1}{2}((\beta+\lambda)(2\beta+\lambda)-2\kappa)E_1$$

$$E_1^a=\left\langle\overline{U}_x^2\overline{V}^a\right\rangle\frac{\lambda}{\kappa^2(2\lambda+\eta)}\qquad F_1^a=-\frac{2\eta\lambda+\kappa+3\lambda^2+\lambda_a}{\eta+2\lambda}E_1^a$$

$$F_2^a=\frac{-(\eta+\lambda)(2\eta+3\lambda)+\kappa+\lambda_a}{\eta+2\lambda}E_1^a,\quad C_1^a=\frac{\lambda_a(\eta+\lambda)+\lambda(\eta+\lambda)(2\eta+3\lambda)-\kappa\lambda}{\eta+2\lambda}E_1^a.$$

Recall that $\lambda=\frac{1}{2}\left[\sqrt{\eta^2-4\kappa}-\eta\right]$. Other terms are given by similar formulas.

B.1 Comparison with Regular Perturbation Theory

Next, let's do a sanity check. Let's shift $\omega_{ij}\to\omega^{ij}+\epsilon\omega_1^{ij}$ with ϵ being some small number. In this case we already know the answer because the correction to κ follows from usual perturbation theory:

$$\delta\kappa = \overline{U}^i_x \omega_1^{ij} \overline{U}^j_x, \tag{B.5}$$

where $\overline{U}^i_x \omega_{ij} = \kappa \overline{U}^j_x$.

Let's now check that the above answer agrees with the one using the dynamical prefactor.

As before, one makes the ansatz $\zeta = \zeta_0 + \epsilon\zeta_1\zeta_0'$ where ζ_0 is given in Equation 4.9. After some algebra one finds

$$-T\eta\partial_\pi^2\zeta_1 + \left[\pi^i\partial_x^i + \eta\pi^i\partial_\pi^i - x^i\omega^{ij}\partial_\pi^j + 2\eta T\frac{u}{\gamma}\overline{U}^i_\pi\partial_\pi^i\right]\zeta_1 + \lambda\zeta_1 = \overline{U}^i_\pi\omega_1^{ij}x^j. \tag{B.6}$$

Following the previous section, the ansatz is

$$\zeta_1 = Au + \sum_a A_a V_a^i \pi^i + B_1 \overline{U}^i_x x^i + \sum_a B_a \overline{V}^i_a x^i v_a, \tag{B.7}$$

where V_a^i are eigenvectors of ω^{ij} with positive eigenvalues λ_a. After collecting terms we get

$$\begin{aligned} A &= \frac{\langle \overline{U}_\pi \overline{U}_x\rangle |\kappa|}{2\lambda(\lambda^2+|\kappa|)}, \quad B_1 = \frac{\langle \overline{U}_\pi \overline{U}_x\rangle \lambda}{\lambda^2+|\kappa|}, \\ A_a &= \frac{\langle \overline{U}_\pi \overline{V}^a\rangle}{\lambda_a}, \quad B_a = \frac{\lambda+\eta}{\lambda_a}\langle \overline{U}_\pi \overline{V}^a\rangle. \end{aligned} \tag{B.8}$$

Here I use the shorthand $\langle UV\rangle \equiv U^i\omega_1^{ij}V^j$.

Just as in the overdamped case, the rate involves integrating at a surface normal to u. Since eigenvectors are orthogonal, all A_a and B_a terms drop out.

Adding ζ_1 changes the rate by

$$\delta\Gamma = -\frac{1}{8\pi}\langle \overline{U}^2_x\rangle\left(\frac{4}{\sqrt{\eta^2+4\omega^2}} - \frac{2}{\eta}\right)|\det\omega|^{-1/2}e^{-V_B/T} \tag{B.9}$$

With ζ_1 taken care of, this still leaves contributions from the Boltzmann factor. This contribution is

$$\delta\Gamma = -\frac{\langle \overline{U}^2_x\rangle}{2\pi}\frac{\left(\eta-\sqrt{\eta^2+4\omega^2}\right)^2}{8\eta\omega^2}|\det\omega|^{-1/2}e^{-V_B/T}. \tag{B.10}$$

Adding these two contributions together is equivalent to taking $|\kappa| \to |\kappa| - \langle \overline{U}^2_x\rangle$ in

$$j = \frac{\lambda}{2\pi}|\det\omega|^{-1/2}e^{-V_B/T}. \tag{B.11}$$

So our result agrees with regular perturbation theory.

C Dynamical Prefactor for Dimension 6 Operators

Recall Equation 3.26

$$T\partial_i^2\zeta_1 + \partial_i\zeta_1\left[2\kappa u\overline{U}^i - \omega^{ij}x_j\right] + \kappa\zeta_1 = \left\langle \overline{U}x^2\right\rangle + \left\langle \overline{U}x^3\right\rangle, \tag{C.1}$$

where the ansatz was

$$\zeta_1 = A + B_1 u + B_a v_a + C_1 u^2 + C_a u v_a + C_{ab} v_{ab} + D_1 u^3 + D_a u^2 v_a + D_{ab} u v_{ab} + D_{abc} v_{abc}.$$

Here I try to not clutter the pages and use $v_{abc} \equiv v_a v_b v_c$ and $\left\langle \overline{V}_{abc}\right\rangle \equiv \left\langle \overline{V}_a\overline{V}_b\overline{V}_c\right\rangle$;all repeated indices are summed over.

Identifying terms one finds ($\lambda_{ab\dots} \equiv \lambda_a + \lambda_b + \dots$)

$$\begin{aligned}
&D_{abc} = \left\langle \overline{UV}_{abc}\right\rangle(\kappa - \lambda_{abc})^{-1}, && D_{ab} = 3\left\langle \overline{U}^2\overline{V}_{ab}\right\rangle(2\kappa - \lambda_{ab})^{-1},\\
&D_a = 3\left\langle \overline{U}^3\overline{V}_a\right\rangle(3\kappa - \lambda_a)^{-1}, && D_1 = \left\langle \overline{U}^4\right\rangle(4\kappa)^{-1},\\
&C_{ab} = \left\langle \overline{UV}_{ab}\right\rangle(\kappa - \lambda_{ab})^{-1}, && C_a = 2\left\langle \overline{U}^2\overline{V}_a\right\rangle(2\kappa - \lambda_a)^{-1},\\
&C_1 = \left\langle \overline{U}^3\right\rangle(3\kappa)^{-1}, && B_1 = -T(2\kappa)^{-1}(6D_1 + 2D_{aa}),\\
&B_a = -T\kappa^{-1}(6D_{acc}), && A = -T\kappa^{-1}(2C_{aa} + 2C_1).
\end{aligned} \tag{C.2}$$

Consider now a potential

$$\overline{U}^i\partial_i V = \left\langle \overline{U}x^2\right\rangle + \left\langle \overline{U}x^3\right\rangle + \left\langle \overline{U}x^4\right\rangle + \left\langle \overline{U}x^5\right\rangle. \tag{C.3}$$

In the language of SM-EFT the above potential would correspond to including a dimension 6 operator in the tree-level Lagrangian. See [46].

This new potential necessitates including the terms

$$\begin{aligned}
\delta\zeta_1 &= E_1 u^4 + E_a u^3 v_a + E_{ab} u^2 v_{ab} + E_{abc} u v_{abc} + E_{abcd} v_{abcd}\\
&\quad + F_1 u^5 + F_a u^4 v_a + F_{ab} u^3 v_{ab} + F_{abc} u^2 v_{abc} + u F_{abcd} v_{abcd} + F_{abcde} v_{abcde}.
\end{aligned} \tag{C.4}$$

One finds

$$\begin{aligned}
&F_1 = (6\kappa)^{-1}\left\langle \overline{U}^6\right\rangle, && E_1 = (5\kappa)^{-1}\left\langle \overline{U}^5\right\rangle,\\
&F_a = (5\kappa - \lambda_a)^{-1}\left\langle \overline{U}^5\overline{V}_a\right\rangle, && E_a = (4\kappa - \lambda_a)^{-1}\left\langle \overline{U}^4\overline{V}_a\right\rangle,\\
&F_{ab} = (4\kappa - \lambda_{ab})^{-1}\left\langle \overline{U}^4\overline{V}_{ab}\right\rangle, && E_{ab} = (3\kappa - \lambda_{ab})^{-1}\left\langle \overline{U}^3\overline{V}_{ab}\right\rangle,\\
&F_{abc} = (3\kappa - \lambda_{abc})^{-1}\left\langle \overline{U}^3\overline{V}_{abc}\right\rangle, && E_{abc} = (2\kappa - \lambda_{abc})^{-1}\left\langle \overline{U}^2\overline{V}_{abc}\right\rangle,\\
&F_{abcd} = (2\kappa - \lambda_{abcd})^{-1}\left\langle \overline{U}^2\overline{V}_{abcd}\right\rangle, && E_{abcd} = (\kappa - \lambda_{abcd})^{-1}\left\langle \overline{U}^1\overline{V}_{abcd}\right\rangle,\\
&F_{abcde} = (\kappa - \lambda_{abcde})^{-1}\left\langle \overline{U}^1\overline{V}_{abcde}\right\rangle.
\end{aligned} \tag{C.5}$$

Remaining terms are given by Equation C.2 with the modification

$$\begin{aligned} &\delta D_{abc} = -5\times 4F_{abcee} - 2F_{abc}, && D_{ab} = -4\times 3F_{abee} - 3\times 2F_{ab},\\ &D_a = -3\times 2F_{aee} - 4\times 3F_a, && D_1 = -2F_{ee} - 5\times 4F_1,\\ &\delta C_{ab} = -4\times 3E_{abee} - 2E_{ab}, && \delta C_a = -3\times 2E_{aee} - 3\times 2E_a,\\ &\delta C_1 = -2E_{ee} - 4\times 3E_1. \end{aligned} \tag{C.6}$$

The above factors, once included in the rate, can be written in terms of propagators. See Section 5 for the details.

D Higher-Order corrections to the Dynamical Prefactor

Here I determine the ζ_2 term in the ansatz

$$\zeta = \zeta_0 + \zeta_1\zeta_0' + \zeta_2\zeta_0' + \ldots \tag{D.1}$$

Assuming $\overline{U}^i\partial_i V = \langle \overline{U}x^2\rangle + \langle \overline{U}x^3\rangle$, we get the equation

$$\begin{aligned} T\partial_i^2\zeta_2 + \partial_i\zeta_2\left[2\kappa u\overline{U}^i - \omega^{ij}x_j\right] + \kappa\zeta_2 = \left(\kappa\frac{u}{T}\zeta_1 + \partial_u\zeta_1\right)\left(\langle \overline{U}x^2\rangle + \langle \overline{U}x^3\rangle\right)\\ + \sum_a \frac{\partial}{\partial v_a}\zeta_1\left(\langle \overline{V}^a x^2\rangle + \langle \overline{V}^a x^3\rangle\right), \end{aligned} \tag{D.2}$$

where ζ_1 is given in Equation C.2. Note that in solving this equation, much work can be recycled from Section C. The ansatz is

$$\begin{aligned} \zeta_2 = {} & A + B_1u + B_av_a + C_1u^2 + C_auv_a + C_{ab}v_{ab} + D_1u^3 + D_au^2v_a + D_{ab}uv_{ab} + D_{abc}v_{abc}\\ & E_1u^4 + E_au^3v_a + E_{ab}u^2v_{ab} + E_{abc}uv_{abc} + E_{abcd}v_{abcd}\\ & + F_1u^5 + F_au^4v_a + F_{ab}u^3v_{ab} + F_{abc}u^2v_{abc} + uF_{abcd}v_{abcd} + F_{abcde}v_{abcde}\\ & + G_1u^6 + G_au^5v_a + G_{ab}u^4v_{ab} + G_{abc}u^3v_{abc} + u^2G_{abcd}v_{abcd} + uG_{abcde}v_{abcde}.\\ & + H_1u^7 + H_au^6v_a + H_{ab}u^5v_{ab} + H_{abc}u^4v_{abc} + u^3H_{abcd}v_{abcd} + u^2H_{abcde}v_{abcde} + uH_{abcdef}v_{abcdef}. \end{aligned}$$

Most of these terms were given in Appendix C. Only the G and H terms are new. These are however readily found[27]

$$\begin{aligned} H_1 &= (8\kappa)^{-1}\kappa^{-1}D_1\left\langle \overline{U}^4\right\rangle\\ H_a &= (7\kappa-\lambda_a)^{-1}\kappa^{-1}\left[3D_1\left\langle \overline{U}^3\overline{V}_a\right\rangle + D_a\left\langle \overline{U}^4\right\rangle\right]\\ H_{ab} &= (6\kappa-\lambda_{ab})^{-1}\kappa^{-1}\left[3D_1\left\langle \overline{U}^2\overline{V}_{ab}\right\rangle + 3D_a\left\langle \overline{U}^3\overline{V}_a\right\rangle + D_{ab}\left\langle \overline{U}^4\right\rangle\right]\\ H_{abc} &= (5\kappa-\lambda_{abc})^{-1}\kappa^{-1}\left[D_1\left\langle \overline{UV}_{abc}\right\rangle + 3D_a\left\langle \overline{U}^2\overline{V}_{bc}\right\rangle + 3D_{ab}\left\langle \overline{U}^3\overline{V}_c\right\rangle + D_{abc}\left\langle \overline{U}^4\right\rangle\right]\\ H_{abcd} &= (4\kappa-\lambda_{abcd})^{-1}\kappa^{-1}\left[D_a\left\langle \overline{UV}_{bcd}\right\rangle + 3D_{ab}\left\langle \overline{U}^2\overline{V}_{cd}\right\rangle + 3D_{abc}\left\langle \overline{U}^3\overline{V}_d\right\rangle\right]\\ H_{abcde} &= (3\kappa-\lambda_{abcde})^{-1}\kappa^{-1}\left[D_{ab}\left\langle \overline{UV}_{cde}\right\rangle + 3D_{abc}\left\langle \overline{U}^2\overline{V}_{de}\right\rangle\right]\\ H_{abcdef} &= (2\kappa-\lambda_{abcdef})^{-1}\kappa^{-1}\left[D_{abc}\left\langle \overline{UV}_{def}\right\rangle\right] \end{aligned}$$

27 All of these expressions should be symmetrised (completely symmetric) in their respective indices.

$$
\begin{aligned}
G_1 &= (7\kappa)^{-1}\kappa^{-1}\left[D_1\left\langle\overline{U}^3\right\rangle + C_1\left\langle\overline{U}^4\right\rangle\right],\\
G_a &= (6\kappa-\lambda_a)^{-1}\kappa^{-1}\left[2D_1\left\langle\overline{U}^2\overline{V}_a\right\rangle + 3C_1\left\langle\overline{U}^3\overline{V}^a\right\rangle + D_a\left\langle\overline{U}^3\right\rangle + C_a\left\langle\overline{U}^4\right\rangle\right],\\
G_{ab} &= (5\kappa-\lambda_{ab})^{-1}\kappa^{-1}\left[D_1\left\langle\overline{UV}_{ab}\right\rangle + 3C_1\left\langle\overline{U}^2\overline{V}_{ab}\right\rangle + 2D_a\left\langle\overline{U}^2\overline{V}_b\right\rangle + 3C_a\left\langle\overline{U}^3\overline{V}_b\right\rangle + C_{ab}\left\langle\overline{U}^4\right\rangle + D_{ab}\left\langle\overline{U}^3\right\rangle\right],\\
G_{abc} &= (4\kappa-\lambda_{abc})^{-1}\kappa^{-1}\left[C_1\left\langle\overline{UV}_{abc}\right\rangle + D_a\left\langle\overline{UV}_{bc}\right\rangle + 3C_a\left\langle\overline{U}^2\overline{V}_{bc}\right\rangle\right.\\
&\qquad\qquad\left. +3C_{ab}\left\langle\overline{U}^3\overline{V}_c\right\rangle + 2D_{ab}\left\langle\overline{U}^2\overline{V}_c\right\rangle + D_{abc}\left\langle\overline{U}^3\right\rangle\right],\\
G_{abcd} &= (3\kappa-\lambda_{abcd})^{-1}\kappa^{-1}\left[C_a\left\langle\overline{UV}_{bcd}\right\rangle + 3C_{ab}\left\langle\overline{U}^2\overline{V}_{cd}\right\rangle + D_{ab}\left\langle\overline{UV}_{cd}\right\rangle + 2D_{abc}\left\langle\overline{U}^2\overline{V}_d\right\rangle\right],\\
G_{abcde} &= (2\kappa-\lambda_{abcde})^{-1}\kappa^{-1}\left[C_{ab}\left\langle\overline{UV}_{cde}\right\rangle + D_{abc}\left\langle\overline{UV}_{de}\right\rangle\right].
\end{aligned}
$$

Remaining terms are given via Equation C.4. These expressions are rather lengthy, so here I only write out those relevant for the NLO dynamical prefactor as discussed in Section 3.3.

Terms that involve two cubic vertices—and so relevant at NLO—are

$$
\begin{aligned}
D_1 =& -\frac{5}{18}\kappa^{-2}\left\langle\overline{U}^3\right\rangle^2 - \frac{2}{3}\kappa^{-1}\frac{1}{\kappa-\lambda_{cc}}\left\langle\overline{U}^3\right\rangle\left\langle\overline{UV}^{cc}\right\rangle\\
&-\frac{\lambda_c}{2\kappa}\frac{1}{(2\kappa-\lambda_c)^2}\left\langle\overline{U}^2\overline{V}^c\right\rangle\left\langle\overline{U}^2\overline{V}^c\right\rangle,\\
D_{ab} =& -2\frac{1}{(\kappa-\lambda_{ab})(2\kappa-\lambda_{ab})}\left\langle\overline{U}^3\right\rangle\left\langle\overline{UV}^{ab}\right\rangle\\
&-2\frac{2\kappa+\lambda_{ab}}{(2\kappa-\lambda_a)(2\kappa-\lambda_b)(2\kappa-\lambda_{ab})}\left\langle\overline{U}^2\overline{V}^a\right\rangle\left\langle\overline{U}^2\overline{V}^b\right\rangle\\
&\;2\frac{1}{(2\kappa-\lambda_c)(2\kappa-\lambda_{ab})}\left\langle\overline{U}^2\overline{V}^c\right\rangle\left\langle\overline{V}^c\overline{V}^{ab}\right\rangle\\
&-2\frac{1}{(\kappa-\lambda_{ab})(\kappa-\lambda_{cc})}\left\langle\overline{UV}^{ab}\right\rangle\left\langle\overline{UV}^{cc}\right\rangle\\
&-2\frac{\lambda_{ab}+\lambda_{cc}}{(2\kappa-\lambda_{ab}-\lambda_{cc})(2\kappa-\lambda_{ab})}\left(\frac{1}{\kappa-\lambda_{ac}}+\frac{1}{\kappa-\lambda_{bc}}\right)\left\langle\overline{UV}^{ac}\right\rangle\left\langle\overline{UV}^{bc}\right\rangle,\\
F_{abcd} =& (3!)^{-1}\frac{\kappa}{T}\frac{1}{(2\kappa-\lambda_{abcd})}\left[\frac{1}{\kappa-\lambda_{ab}}\left\langle\overline{UV}^{ab}\right\rangle\left\langle\overline{UV}^{cd}\right\rangle + \frac{1}{\kappa-\lambda_{cd}}\left\langle\overline{UV}^{ab}\right\rangle\left\langle\overline{UV}^{cd}\right\rangle\right.\\
&\qquad 2\frac{1}{\kappa-\lambda_{ac}}\left\langle\overline{UV}^{ac}\right\rangle\left\langle\overline{UV}^{bd}\right\rangle + \frac{1}{\kappa-\lambda_{ad}}\left\langle\overline{UV}^{ad}\right\rangle\left\langle\overline{UV}^{bc}\right\rangle\\
&\qquad\left.+\frac{1}{\kappa-\lambda_{bc}}\left\langle\overline{UV}^{ad}\right\rangle\left\langle\overline{UV}^{bc}\right\rangle + \frac{1}{\kappa-\lambda_{bd}}\left\langle\overline{UV}^{bd}\right\rangle\left\langle\overline{UV}^{ac}\right\rangle\right],\\
B_1 =& -T(2\kappa)^{-1}(6D_1+2D_{aa}).
\end{aligned}
\tag{D.3}
$$

All formulas use the notation $\lambda_{ab\ldots}=\lambda_a+\lambda_b+\ldots$; $\overline{V}^{ab\ldots}=\overline{V}^a\overline{V}^b\ldots$; and repeated indices are summed over *only* once—the sum does not include the negative eigenvalue κ.

To calculate the rate we need to perform Wick contractions of F_{abcd}, D_{ab}, and B_1. This gives

$$
\delta A_{\text{dyn}} = \frac{\sqrt{|\kappa|}}{2\pi\eta}\left[3F_{aabb}\lambda_a^{-1}\lambda_b^{-1} + D_{aa}\lambda_a^{-1} + B_1\right]. \tag{D.4}
$$

After the smoke settles one finds

$$\begin{aligned}\delta A_{\text{dyn}} =&\frac{\sqrt{|\kappa|}}{2\pi\eta}T\Bigg[\frac{5}{6}\kappa^{-3}\left\langle\overline{U}^3\right\rangle^2-\kappa^{-2}\lambda_a^{-1}\left\langle\overline{U}^3\right\rangle\left\langle\overline{UV}^{aa}\right\rangle+\kappa^{-2}\left(\frac{2}{\lambda_a-2\kappa}-\frac{1}{2\lambda_a}\right)\left\langle\overline{U}^2\overline{V}^a\right\rangle\left\langle\overline{U}^2\overline{V}^a\right\rangle\\&+\kappa^{-1}\lambda_a^{-1}(2\kappa-\lambda_c)^{-1}\left\langle\overline{U}^2\overline{V}^c\right\rangle\left\langle\overline{V}^c\overline{V}^{aa}\right\rangle-\kappa^{-1}\frac{\kappa+\lambda_{ab}}{\lambda_a\lambda_b(\lambda_{ab}-\kappa)}\left\langle\overline{UV}^{ab}\right\rangle\left\langle\overline{UV}^{ab}\right\rangle\\&+\kappa^{-1}\frac{1}{2}\lambda_a^{-1}\lambda_b^{-1}\left\langle\overline{UV}^{aa}\right\rangle\left\langle\overline{UV}^{cc}\right\rangle\Bigg].\end{aligned}\tag{D.5}$$

Or written in terms of propagators

$$\begin{aligned}\delta A_{\text{dyn}} = \frac{\sqrt{|\kappa|}}{2\pi\eta}T\Bigg[&\frac{23}{6}\kappa^{-3}\left\langle\overline{U}^3\right\rangle^2-\kappa^{-2}\left\langle\overline{U}\right\rangle^3\left\langle\overline{U}\Delta_{2\kappa}\right\rangle-3\kappa^{-2}\left\langle\overline{U}^3\right\rangle\left\langle\overline{U}\Delta\right\rangle+3\kappa^{-2}\left\langle\overline{U}^2\Delta_k\overline{U}^2\right\rangle\\&+\frac{3}{2}\kappa^{-2}\left\langle\overline{U}^2\Delta\overline{U}^2\right\rangle+\kappa^{-1}\left\langle\overline{U}\Delta\right\rangle^2-\kappa^{-1}\left\langle\overline{U}\Delta^2\overline{U}\right\rangle-\kappa^{-1}\left\langle\overline{U}^2\Delta_{2\kappa}\Delta\right\rangle\Bigg].\end{aligned}$$

Here $\left\langle\overline{U}^2\Delta\overline{U}^2\right\rangle\equiv\lambda_3^{ijk}\overline{U}^i\overline{U}^j\Delta^{kl}\lambda_3^{lnm}\overline{U}^n\overline{U}^m$ and $\left\langle\overline{U}\Delta\Delta\overline{U}\right\rangle\equiv\lambda_3^{ijk}\overline{U}^i\Delta^{jl}\Delta^{kn}\lambda_3^{lnm}\overline{U}^m$.

For field theory the equivalent expression is

$$\begin{aligned}\delta A_{\text{dyn}} =&\Bigg[\frac{23}{24}\kappa^{-3}\left(\int d^3x\overline{U}(x)^3(\lambda\phi_b(x)-g)\right)^2-\frac{1}{4}\kappa^{-2}\int d^3xd^3y\overline{U}(x)^3\overline{U}(y)\Delta_{2\kappa}(y,y)A(x,y)\\&-\frac{5}{4}\kappa^{-2}\int d^3xd^3y\overline{U}(x)^3\overline{U}(y)\Delta(y,y)A(x,y)\\&\frac{3}{4}\kappa^{-2}\int d^3xd^3y\overline{U}(x)^2\left(\Delta_{2\kappa}(x,y)+\frac{1}{2}\Delta(x,y)\right)\overline{U}(y)^2A(x,y)\\&\frac{1}{4}\kappa^{-1}\left(\int d^3x\overline{U}(x)\Delta(x,x)(\lambda\phi_b(x)-g)\right)^2\\&-\frac{1}{4}\int d^3xd^3y\overline{U}(x)\Delta(x,y)^2\overline{U}(y)A(x,y)\\&-\frac{1}{4}\kappa^{-1}\int d^3xd^3y\overline{U}(x)^2\Delta_{2\kappa}(x,y)\Delta(y,y)\Bigg].\end{aligned}\tag{D.6}$$

E WKB Approximation for Large l

In this section I want to approximate the propagator for large l. To that end, consider Equation 6.3 with $r \neq r'$. Rewrite this Equation with Langer's ansatz [85] $\Delta(r,r') = e^{ax}\Psi(r=e^x)$. Essentially this ansatz eliminates the ∂_r term in Equation 6.3 and makes a WKB ansatz possible. I here work in $d = 3-2\epsilon$ dimensions to regulate all $\vec{x} \to \vec{y}$ divergences. The equation for $\Psi(x)$ is [86–88]

$$\begin{aligned}&\Psi''(x)-A(x)\Psi(x)=0,\\&A(x)=e^{2x}V''[\phi_b(e^x)]+\bar{l}^2,\\&\bar{l}=\frac{d+2l-2}{2}.\end{aligned}\tag{E.1}$$

Making a WKB ansatz [85, 89, 90] one finds

$$\Delta_l^{>}(r,r') = r^{-(d-2)/2}\frac{1}{\sqrt{\bar{l}}}r^{-\bar{l}}\left[A^{>}(r')e^{-S_0(r)}\right], \tag{E.2}$$

$$\Delta_l^{<}(r,r') = r^{-(d-2)/2}\frac{1}{\sqrt{\bar{l}}}r^{\bar{l}}\left[A^{<}(r')e^{S_0(r)}\right], \tag{E.3}$$

where $S_0[r] = \frac{1}{2\bar{l}}\int_0^r dx x V''[\phi_b(x)]$. Here $\delta_l^{>}(r,r')$ is defined with $r > r'$ and $\delta_l^{<}(r,r')$ with $r < r'$.

I here did two things. First, I expanded in powers of $\bar{l}$, second, I used boundary conditions to ensure that $\Delta_l^{>}(r,r')$ is finite in the $r \to \infty$ limit, and that $\Delta_l^{<}(r,r')$ is finite in the $r \to 0$ limit.

The actual Green's function is found by demanding

$$\left[\Delta^{>}(r,r') - \Delta^{<}(r,r')\right]_{r=r'} = 0, \tag{E.4}$$

$$\left[\partial_r\Delta^{>}(r,r') - \partial_r\Delta^{<}(r,r')\right]_{r=r'} = 1/(r')^{d-1}. \tag{E.5}$$

Doing the matching one finds the propagator

$$\Delta_l(r,r') = \begin{cases} \frac{(r')^l r^{-d-l+2}}{d+2l-2} - \frac{(r')^l}{r^{2-d-l}}\frac{(d+2l-2)\left[f(r)-f(r')\right]+r^2W(r)+(r')^2W(r')}{(d+2l-2)^3} & \text{if } r > r' \\ \frac{r^l(r')^{-d-l+2}}{d+2l-2} - \frac{(r)^l}{(r')^{2-d-l}}\frac{(d+2l-2)\left[f(r')-f(r)\right]+r^2W(r)+(r')^2W(r')}{(d+2l-2)^3} & \text{if } r < r' \end{cases} \tag{E.6}$$

Here $W(r) \equiv V''[\phi_b(r)]$ and $f(r) \equiv \int_0^r ds s W(s)$.

The $l = L+1, \ldots, \infty$ sum is now straightforward, and the leading result is given in Equation 6.2. The next-to-leading result is

$$\delta_1 = \begin{cases} \frac{2f(|x|)\log\left(\frac{-2\sqrt{|x|y}+|x|+|y|}{|x|-|y|}\right)+4f(|y|)\tanh^{-1}\left(\sqrt{\frac{|y|}{|x|}}\right)+\left(\mathrm{Li}_2\left(\frac{|y|}{|x|}\right)-4\mathrm{Li}_2\left(\sqrt{\frac{|y|}{|x|}}\right)\right)\left(|x|^2W(|x|)+|y|^2W(|y|)\right)}{16\pi\sqrt{|x||y|}} & \text{if } |x| > |y| \\ \frac{2f(|y|)\log\left(\frac{-2\sqrt{|x||y|}+|x|+|y|}{|y|-|x|}\right)+4f(|x|)\tanh^{-1}\left(\sqrt{\frac{|x|}{|y|}}\right)+\left(\mathrm{Li}_2\left(\frac{|x|}{|y|}\right)-4\mathrm{Li}_2\left(\sqrt{\frac{|x|}{|y|}}\right)\right)\left(|x|^2W(|x|)+|y|^2W(|y|)\right)}{16\pi\sqrt{|x||y|}} & \text{if } |x| < |y| \end{cases}$$

References

[1] J. S. Langer, "Statistical theory of the decay of metastable states," *Annals Phys.* **54** (1969) 258–275.

[2] H. Kramers, "Brownian motion in a field of force and the diffusion model of chemical reactions," *Physica* **7** (1940) 284–304.

[3] J. S. Langer and L. A. Turski, "Hydrodynamic model of the condensation of a vapor near its critical point," *Phys. Rev. A* **8** (Dec, 1973) 3230–3243.

[4] D. Bodeker, "From hard thermal loops to Langevin dynamics," *Nucl. Phys. B* **559** (1999) 502–538, arXiv:hep-ph/9905239.

[5] P. B. Arnold, D. T. Son, and L. G. Yaffe, "Effective dynamics of hot, soft nonAbelian gauge fields. Color conductivity and log(1/alpha) effects," *Phys. Rev. D* **59** (1999) 105020, arXiv:hep-ph/9810216.

[6] J. P. Blaizot and E. Iancu, "Kinetic equations for long wavelength excitations of the quark - gluon plasma," *Phys. Rev. Lett.* **70** (1993) 3376–3379, arXiv:hep-ph/9301236.

[7] G. D. Moore and K. Rummukainen, "Electroweak bubble nucleation, nonperturbatively," *Phys. Rev. D* **63** (2001) 045002, arXiv:hep-ph/0009132.

[8] G. D. Moore, "Measuring the broken phase sphaleron rate nonperturbatively," *Phys. Rev. D* **59** (1999) 014503, arXiv:hep-ph/9805264.

[9] A. Andreassen, D. Farhi, W. Frost, and M. D. Schwartz, "Precision decay rate calculations in quantum field theory," *Phys. Rev. D* **95** (2017) 085011, arXiv:1604.06090 [hep-th].

[10] A. Andreassen, W. Frost, and M. D. Schwartz, "Scale Invariant Instantons and the Complete Lifetime of the Standard Model," *Phys. Rev. D* **97** (2018) 056006, arXiv:1707.08124 [hep-ph].

[11] J. Gervals, A. Jevicki, and B. Sakita, "Viii. collective coordinate method for quantization of extended systems," *Physics Reports* **23** (1976) 281–293.

[12] J. P. Blaizot and E. Iancu, "Soft collective excitations in hot gauge theories," *Nucl. Phys. B* **417** (1994) 608–673, arXiv:hep-ph/9306294.

[13] A. Berera, I. G. Moss, and R. O. Ramos, "Local Approximations for Effective Scalar Field Equations of Motion," *Phys. Rev. D* **76** (2007) 083520, arXiv:0706.2793 [hep-ph].

[14] F. Gautier and J. Serreau, "Langevin description of nonequilibrium quantum fields," *Phys. Rev. D* **86** (Dec, 2012) 125002.

[15] **LIGO Scientific, Virgo** Collaboration, B. P. Abbott *et al.*, "Observation of Gravitational Waves from a Binary Black Hole Merger," *Phys. Rev. Lett.* **116** (2016) 061102, arXiv:1602.03837 [gr-qc].

[16] M. B. Hindmarsh, M. Lüben, J. Lumma, and M. Pauly, "Phase transitions in the early universe," *SciPost Phys. Lect. Notes* **24** (2021) 1, arXiv:2008.09136 [astro-ph.CO].

[17] H.-K. Guo, K. Sinha, D. Vagie, and G. White, "The Benefits of Diligence: How Precise are Predicted Gravitational Wave Spectra in Models with Phase Transitions?," arXiv:2103.06933 [hep-ph].

[18] C. Caprini *et al.*, "Detecting gravitational waves from cosmological phase transitions with LISA: an update," *JCAP* **03** (2020) 024, arXiv:1910.13125 [astro-ph.CO].

[19] V. A. Kuzmin, V. A. Rubakov, and M. E. Shaposhnikov, "On the Anomalous Electroweak Baryon Number Nonconservation in the Early Universe," *Phys. Lett. B* **155** (1985) 36.

[20] M. E. Shaposhnikov, "Possible Appearance of the Baryon Asymmetry of the Universe in an Electroweak Theory," *JETP Lett.* **44** (1986) 465–468.

[21] M. E. Shaposhnikov, "Baryon Asymmetry of the Universe in Standard Electroweak Theory," *Nucl. Phys. B* **287** (1987) 757–775.

[22] A. G. Cohen, D. B. Kaplan, and A. E. Nelson, "Progress in electroweak baryogenesis," *Ann. Rev. Nucl. Part. Sci.* **43** (1993) 27–70, arXiv:hep-ph/9302210.

[23] A. D. Linde, "Decay of the False Vacuum at Finite Temperature," *Nucl. Phys. B* **216** (1983) 421.

[24] S. R. Coleman and F. De Luccia, "Gravitational Effects on and of Vacuum Decay," *Phys. Rev. D* **21** (1980) 3305.

[25] C. G. Callan, Jr. and S. R. Coleman, "The Fate of the False Vacuum. 2. First Quantum Corrections," *Phys. Rev. D* **16** (1977) 1762–1768.

[26] S. R. Coleman, "The Fate of the False Vacuum. 1. Semiclassical Theory," *Phys. Rev. D* **15** (1977) 2929–2936.

[27] C. Caprini and R. Durrer, "Gravitational waves from stochastic relativistic sources: Primordial turbulence and magnetic fields," *Phys. Rev. D* **74** (2006) 063521, arXiv:astro-ph/0603476.

[28] M. Hindmarsh, S. J. Huber, K. Rummukainen, and D. J. Weir, "Shape of the acoustic gravitational wave power spectrum from a first order phase transition," *Phys. Rev. D* **96** (2017) 103520, arXiv:1704.05871 [astro-ph.CO].

[29] M. Hindmarsh, S. J. Huber, K. Rummukainen, and D. J. Weir, "Numerical simulations of acoustically generated gravitational waves at a first order phase transition," *Phys. Rev. D* **92** (Dec, 2015) 123009.

[30] M. Hindmarsh, S. J. Huber, K. Rummukainen, and D. J. Weir, "Gravitational waves from the sound of a first order phase transition," *Phys. Rev. Lett.* **112** (2014) 041301, arXiv:1304.2433 [hep-ph].

[31] R. Jinno and M. Takimoto, "Gravitational waves from bubble collisions: An analytic derivation," *Phys. Rev. D* **95** (2017) 024009, arXiv:1605.01403 [astro-ph.CO].

[32] e. a. Amaro-Seoane, "Laser Interferometer Space Antenna," *arXiv e-prints* (Feb., 2017) arXiv:1702.00786, arXiv:1702.00786.

[33] W.-H. Ruan, Z.-K. Guo, R.-G. Cai, and Y.-Z. Zhang, "Taiji program: Gravitational-wave sources," *Int. J. Mod. Phys. A* **35** (2020) 2050075, arXiv:1807.09495 [gr-qc].

[34] S. Kawamura *et al.*, "The Japanese space gravitational wave antenna DECIGO," *Class. Quant. Grav.* **23** (2006) S125–S132.

[35] G. M. Harry, P. Fritschel, D. A. Shaddock, W. Folkner, and E. S. Phinney, "Laser interferometry for the big bang observer," *Class. Quant. Grav.* **23** (2006) 4887–4894.

[36] N. Turok and J. Zadrozny, "Phase transitions in the two doublet model," *Nucl. Phys. B* **369** (1992) 729–742.

[37] P. Athron, C. Balazs, A. Fowlie, G. Pozzo, G. White, and Y. Zhang, "Strong first-order phase transitions in the NMSSM — a comprehensive survey," *JHEP* **11** (2019) 151, arXiv:1908.11847 [hep-ph].

[38] V. Barger, P. Langacker, M. McCaskey, M. J. Ramsey-Musolf, and G. Shaughnessy, "LHC Phenomenology of an Extended Standard Model with a Real Scalar Singlet," *Phys. Rev. D* **77** (2008) 035005, arXiv:0706.4311 [hep-ph].

[39] A. Alves, T. Ghosh, H.-K. Guo, K. Sinha, and D. Vagie, "Collider and Gravitational Wave Complementarity in Exploring the Singlet Extension of the Standard Model," *JHEP* **04** (2019) 052, arXiv:1812.09333 [hep-ph].

[40] L. Niemi, P. Schicho, and T. V. I. Tenkanen, "Singlet-assisted electroweak phase transition at two loops," arXiv:2103.07467 [hep-ph].

[41] N. F. Bell, M. J. Dolan, L. S. Friedrich, M. J. Ramsey-Musolf, and R. R. Volkas, "A Real Triplet-Singlet Extended Standard Model: Dark Matter and Collider Phenomenology," arXiv:2010.13376 [hep-ph].

[42] L. Niemi, M. Ramsey-Musolf, T. V. I. Tenkanen, and D. J. Weir, "Thermodynamics of a two-step electroweak phase transition," arXiv:2005.11332 [hep-ph].

[43] J. de Vries, M. Postma, J. van de Vis, and G. White, "Electroweak Baryogenesis and the Standard Model Effective Field Theory," *JHEP* **01** (2018) 089, arXiv:1710.04061 [hep-ph].

[44] E. Hall, T. Konstandin, R. McGehee, H. Murayama, and G. Servant, "Baryogenesis From a Dark First-Order Phase Transition," *JHEP* **04** (2020) 042, arXiv:1910.08068 [hep-ph].

[45] I. Baldes and G. Servant, "High scale electroweak phase transition: baryogenesis and symmetry non-restoration," *JHEP* **10** (2018) 053, arXiv:1807.08770 [hep-ph].

[46] D. Croon, O. Gould, P. Schicho, T. V. I. Tenkanen, and G. White, "Theoretical uncertainties for cosmological first-order phase transitions," arXiv:2009.10080 [hep-ph].

[47] A. Ekstedt, "Higher-Order Corrections to the Bubble-Nucleation Rate at Finite Temperature," arXiv:2104.11804 [hep-ph].

[48] K. Farakos, K. Kajantie, K. Rummukainen, and M. E. Shaposhnikov, "3-D physics and the electroweak phase transition: Perturbation theory," *Nucl. Phys. B* **425** (1994) 67–109, arXiv:hep-ph/9404201.

[49] K. Kajantie, M. Laine, K. Rummukainen, and M. E. Shaposhnikov, "Generic rules for high temperature dimensional reduction and their application to the standard model," *Nucl. Phys. B* **458** (1996) 90–136, arXiv:hep-ph/9508379.

[50] K. Kajantie, M. Laine, K. Rummukainen, and M. E. Shaposhnikov, "The Electroweak phase transition: A Nonperturbative analysis," *Nucl. Phys. B* **466** (1996) 189–258, arXiv:hep-lat/9510020.

[51] K. Rummukainen, K. Kajantie, M. Laine, M. E. Shaposhnikov, and M. Tsypin, "The Universal properties of the electroweak phase transition," 9, 1998. arXiv:hep-ph/9809435.

[52] M. Gurtler, E.-M. Ilgenfritz, and A. Schiller, "Where the electroweak phase transition ends," *Phys. Rev. D* **56** (1997) 3888–3895, arXiv:hep-lat/9704013.

[53] K. Kajantie, M. Laine, K. Rummukainen, and M. E. Shaposhnikov, "Is there a hot electroweak phase transition at m(H) larger or equal to m(W)?," *Phys. Rev. Lett.* **77** (1996) 2887–2890, arXiv:hep-ph/9605288.

[54] O. Gould, "Real scalar phase transitions: a nonperturbative analysis," *JHEP* **04** (2021) 057, arXiv:2101.05528 [hep-ph].

[55] G. C. Dorsch, S. J. Huber, and T. Konstandin, "Bubble wall velocities in the Standard Model and beyond," *JCAP* **12** (2018) 034, arXiv:1809.04907 [hep-ph].

[56] O. Gould, J. Kozaczuk, L. Niemi, M. J. Ramsey-Musolf, T. V. I. Tenkanen, and D. J. Weir, "Nonperturbative analysis of the gravitational waves from a first-order electroweak phase transition," *Phys. Rev. D* **100** (2019) 115024, arXiv:1903.11604 [hep-ph].

[57] J. Löfgren, M. J. Ramsey-Musolf, P. Schicho, and T. V. I. Tenkanen, "Nucleation at finite temperature: a gauge-invariant, perturbative framework," arXiv:2112.05472 [hep-ph].

[58] O. Gould and T. V. I. Tenkanen, "On the perturbative expansion at high temperature and implications for cosmological phase transitions," arXiv:2104.04399 [hep-ph].

[59] J. Baacke and K. Heitmann, "Gauge invariance of the one loop effective action of the Higgs field in the SU(2) Higgs model," *Phys. Rev. D* **60** (1999) 105037, arXiv:hep-th/9905201.

[60] M. Garny and T. Konstandin, "On the gauge dependence of vacuum transitions at finite temperature," *JHEP* **07** (2012) 189, arXiv:1205.3392 [hep-ph].

[61] O. Gould and J. Hirvonen, "Effective field theory approach to thermal bubble nucleation," *Phys. Rev. D* **104** (2021) 096015, arXiv:2108.04377 [hep-ph].

[62] P. B. Arnold and O. Espinosa, “The Effective potential and first order phase transitions: Beyond leading-order,” *Phys. Rev. D* **47** (1993) 3546, arXiv:hep-ph/9212235.

[63] M. E. Carrington and J. I. Kapusta, “Dynamics of the electroweak phase transition,” *Phys. Rev. D* **47** (Jun, 1993) 5304–5315.

[64] I. Affleck, “Quantum Statistical Metastability,” *Phys. Rev. Lett.* **46** (1981) 388.

[65] J. Hirvonen, J. Löfgren, M. J. Ramsey-Musolf, P. Schicho, and T. V. I. Tenkanen, “Computing the gauge-invariant bubble nucleation rate in finite temperature effective field theory,” arXiv:2112.08912 [hep-ph].

[66] S. R. Coleman, “The Uses of Instantons,” *Subnucl. Ser.* **15** (1979) 805.

[67] G. V. Dunne and H. Min, “Beyond the thin-wall approximation: Precise numerical computation of prefactors in false vacuum decay,” *Phys. Rev. D* **72** (2005) 125004, arXiv:hep-th/0511156.

[68] P. Hänggi, P. Talkner, and M. Borkovec, “Reaction-rate theory: fifty years after kramers,” *Rev. Mod. Phys.* **62** (Apr, 1990) 251–341.

[69] A. Linde, “Fate of the false vacuum at finite temperature: Theory and applications,” *Physics Letters B* **100** (1981) 37–40.

[70] A. Linde, “Decay of the false vacuum at finite temperature: A. linde, nucl. phys. b216 (1983) 421,” *Nuclear Physics B* **223** (1983) 544.

[71] A. Berera, J. Mabillard, B. W. Mintz, and R. O. Ramos, “Formulating the Kramers problem in field theory,” *Phys. Rev. D* **100** (2019) 076005, arXiv:1906.08684 [hep-ph].

[72] L. Farkas, “Keimbildungsgeschwindigkeit in übersättigten dämpfen,” *Zeitschrift für Physikalische Chemie* **125U** (1927) 236–242.

[73] A. D. Fokker, “Die mittlere energie rotierender elektrischer dipole im strahlungsfeld,” *Annalen der Physik* **348** (1914) 810–820.

[74] M. V. Smoluchowski, “Über Brownsche Molekularbewegung unter Einwirkung äußerer Kräfte und deren Zusammenhang mit der verallgemeinerten Diffusionsgleichung,” *Annalen der Physik* **353** (Jan., 1915) 1103–1112.

[75] S. Coleman and E. Weinberg, “Radiative corrections as the origin of spontaneous symmetry breaking,” *Phys. Rev. D* **7** (Mar, 1973) 1888–1910.

[76] R. S. Larson and M. D. Kostin, “Kramers’s theory of chemical kinetics: Eigenvalue and eigenfunction analysis,” *The Journal of Chemical Physics* **69** (1978) 4821–4829.

[77] I. Moss, D. Toms, and A. Wright, “Effective actions at finite temperature,” *Phys. Rev. D* **46** (Aug, 1992) 1671–1679.

[78] E. J. Weinberg, “Vacuum decay in theories with symmetry breaking by radiative corrections,” *Phys. Rev. D* **47** (1993) 4614–4627, arXiv:hep-ph/9211314.

[79] E. Braaten and A. Nieto, “Effective field theory approach to high temperature thermodynamics,” *Phys. Rev.* **D51** (1995) 6990–7006, arXiv:hep-ph/9501375 [hep-ph].

[80] A. K. Rajantie, “Feynman diagrams to three loops in three-dimensional field theory,” *Nucl. Phys. B* **480** (1996) 729–752, arXiv:hep-ph/9606216.

[81] M. Fabre de La Ripelle, “Green function and scattering amplitudes in many-dimensional space,” *Few-Body Systems* **14** (Mar., 1993) 1–24.

[82] J. Baacke and S. Junker, "Quantum fluctuations around the electroweak sphaleron," *Phys. Rev. D* **49** (1994) 2055–2073, arXiv:hep-ph/9308310.

[83] L. Carson and L. D. McLerran, "Approximate Computation of the Small Fluctuation Determinant Around a Sphaleron," *Phys. Rev. D* **41** (1990) 647.

[84] F. Gautier and J. Serreau, "On the Langevin description of nonequilibrium quantum fields," *Phys. Rev. D* **86** (2012) 125002, arXiv:1209.1827 [hep-th].

[85] R. E. Langer, "On the Connection Formulas and the Solutions of the Wave Equation," *Phys. Rev.* **51** (1937) 669–676.

[86] G. V. Dunne, J. Hur, C. Lee, and H. Min, "Calculation of QCD instanton determinant with arbitrary mass," *Phys. Rev. D* **71** (2005) 085019, arXiv:hep-th/0502087.

[87] G. V. Dunne and K. Kirsten, "Functional determinants for radial operators," *J. Phys. A* **39** (2006) 11915–11928, arXiv:hep-th/0607066.

[88] G. V. Dunne, J. Hur, and C. Lee, "Renormalized Effective Actions in Radially Symmetric Backgrounds. I. Partial Wave Cutoff Method," *Phys. Rev. D* **74** (2006) 085025, arXiv:hep-th/0609118.

[89] G. Wentzel, "Eine Verallgemeinerung der Quantenbedingungen für die Zwecke der Wellenmechanik," *Z. Phys.* **38** (1926) 518–529.

[90] H. A. Kramers, "Wellenmechanik und halbzahlige Quantisierung," *Z. Phys.* **39** (1926) 828–840.